

## Aerodynamic Properties of Urban Areas Derived from Analysis of Surface Form

C. S. B. GRIMMOND

*Climate and Meteorology Program, Department of Geography, Indiana University at Bloomington,  
Bloomington, Indiana*

T. R. OKE

*Atmospheric Science Program, Department of Geography, University of British Columbia, Vancouver,  
British Columbia, Canada*

(Manuscript received 30 June 1998, in final form 3 December 1998)

### ABSTRACT

Several methods to determine the aerodynamic characteristics of a site through analysis of its surface form (morphometry) are considered in relation to cities. The measures discussed include zero-plane displacement length ( $z_d$ ), roughness length ( $z_0$ ), depth of the roughness sublayer, and aerodynamic conductance. A sensitivity analysis is conducted on seven formulas to estimate  $z_d$  and nine to estimate  $z_0$ , covering a wide range of probable urban roughness densities. Geographic information systems developed for 11 sites in 7 North American cities are used to characterize their morphometry—the height, shape, three-dimensional area, and spatial distribution of their roughness elements (buildings and trees). Most of the sites are in residential suburbs, but one is industrial and two are near city centers. This descriptive survey of urban geometric form is used, together with the morphometric formulas, to derive the apparent aerodynamic characteristics of the sites. The resulting estimates of  $z_d$  and  $z_0$  are compared with values obtained from analysis of wind and turbulence observations. The latter are obtained from a survey of approximately 60 field studies and 14 laboratory studies of real and scale model cities. Despite the comprehensive nature of the survey, very few studies are found to be acceptable and their scatter is large, hence they do not provide a standard against which to test the morphometric algorithms. Further, the data show only weak relations between measured  $z_d$  and  $z_0$  and roughness density. The relative merits of morphometric and wind-based estimates of aerodynamic parameters are discussed. Recommendations are made concerning the choice of method to estimate  $z_d$  and  $z_0$  in urban areas and their most likely magnitude.

### 1. Introduction

Cities are about the roughest surfaces there are, as is evident from scanning any table of zero-plane displacement ( $z_d$ ) or roughness length ( $z_0$ ) values (e.g., Wieringa 1993, Table VIII). This fact has major implications for surface drag, aerodynamic conductance for momentum transport ( $g_{aM}$ ), the scales and intensity of turbulence, mesoscale mass convergence (uplift) and divergence (subsidence), the depths of the roughness sublayer ( $z_r$ ) and Ekman layer, wind speed and the shape of the wind profile, and the type of flow found in the urban canopy layer (Angell et al. 1973; Auer 1981; Landsberg 1981; Cermak et al. 1995). Hence, accurate knowledge of the aerodynamic characteristics of cities is vital to describe, model, and forecast the behavior of urban winds and turbulence at all scales. Unfortunately, our ability to

assign values of  $z_d$  and  $z_0$  remains problematic. Two classes of approach are available:

- 1) *morphometric* (or *geometric*) methods that use algorithms that relate aerodynamic parameters to measures of surface morphometry; and
- 2) *micrometeorological* (or *anemometric*) methods that use field observations of wind or turbulence to solve for aerodynamic parameters included in theoretical relations derived from the logarithmic wind profile.

Morphometric methods have the advantage that values can be determined without need of tall towers and instrumentation. Further, if a spatially continuous database of the distribution of roughness elements is available then values can be computed for any direction surrounding the site of interest. They do, however, have the disadvantage that most are based on empirical relations derived from wind tunnel work that concern idealized flows over simplified arrays of roughness elements. In these simulations the flow is often relatively constant in direction, typically normal to the face of the elements, and the array is often regularly spaced (in

---

*Corresponding author address:* Dr. T. R. Oke, Atmospheric Science Program, Dept. of Geography, University of British Columbia, 1984 West Mall, Vancouver, BC V6T 1Z2, Canada.  
E-mail: toke@geog.ubc.ca

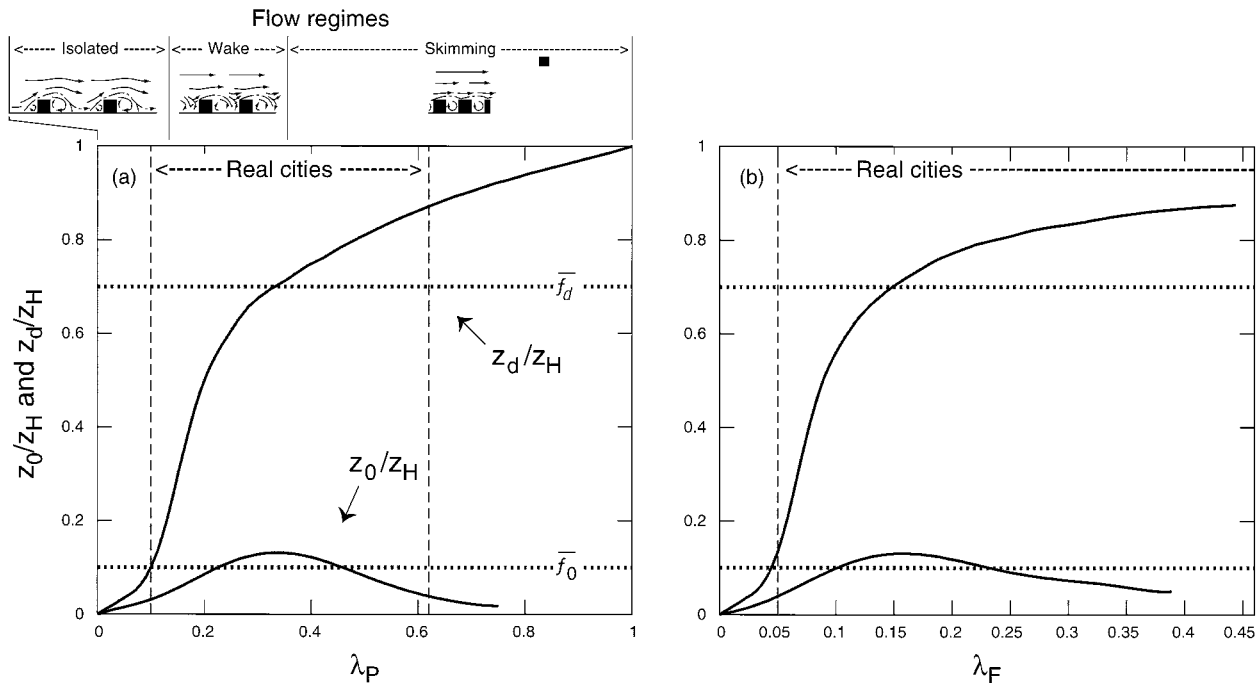


FIG. 1. Conceptual representation of the relation between height-normalized values of zero-plane displacement ( $z_0/z_H$ ) and roughness length ( $z_d/z_H$ ) and the packing density of roughness elements (a) using  $\lambda_p$  and (b) using  $\lambda_F$  to describe density (see Fig. 2 for definitions). Shaded areas are the reasonable zones or envelopes referred to in the text. The range of urban roughness element densities for real cities is based on the combined building and tree values found in this study (Tables 2, 3) and those given by Kratzer (1956) and Theurer (1993) for German cities and Ellefsen (1990–91) for U.S. cities. Mean values of observed  $f_d$  and  $f_0$  [see Eqs. (1) and (2) for definitions] are from Garratt (1992). Limits of flow regimes (along the top) are based on the  $\lambda_s$  values of Hussain and Lee (1980) and are converted to  $\lambda_p$  and  $\lambda_F$  using empirical relations in the present study (appendix A, Fig. A1f, g).

rows or a staggered grid). These conditions differ from those in real cities, where wind direction is ever changing and, even if the street pattern is relatively regular, the size and shape of individual roughness elements (mainly buildings and trees) are not regular.

Wind-based methods have the advantage that the characteristics of the surface do not need to be specified (the roughness elements can consist of any mix and be

arranged in any pattern). The greatest disadvantages are the expense and difficulty involved in obtaining and operating a field site (especially installing a tower in a city), and the fact that, while in principle results can be obtained for any wind direction, in practice appropriate conditions may not occur for all wind directions (e.g., Grimmond et al. 1998).

The following heuristic arguments, illustrated in Fig. 1, provide some quasi-physical reasoning to explain what happens when extra roughness elements are added to a surface, that is, analogous to the growth of a city. We start with a surface of small initial background roughness. Intuition predicts what happens in fully rough flow as tall elements (of height  $z_H$ ) are progressively added, thus increasing the element density. [Note: for simplicity in Fig. 1 we use  $\lambda_p = A_p/A_T$ , the plan area of roughness elements  $A_p$  relative to the total surface area  $A_T$  (see Fig. 2), as the measure of density.] As the density increases so does the roughness of the system, but a point comes where adding new elements merely serves to reduce the effective drag of those already present due to mutual sheltering; that is, they start to “smoother” the roughness of the system. As Shaw and Pereira (1982) note, at this point the increase in drag is offset by an increase in  $z_d$  (see below), which reduces the effective height of the canopy for momentum exchange. This result produces a peak in  $z_0$  at some

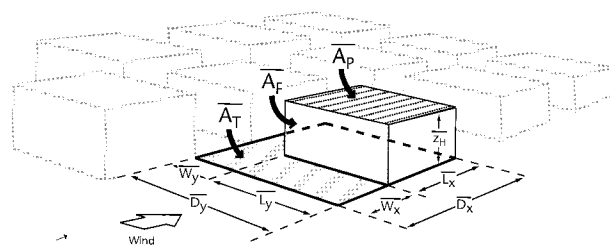


FIG. 2. Definition of surface dimensions used in morphometric analysis. The element portrayed has the characteristic mean dimensions, spacing, and total lot area ( $A_T$ ) of the urban array. Using these measurements, the following nondimensional ratios are defined to characterize the morphometry:  $\lambda_p = A_p/A_T = L_x L_y / D_x D_y$ ,  $\lambda_F = A_p / A_T = z_H L_y / D_x D_y$ ,  $\lambda_s = z_H / W_x = z_H / D_x - L_x$ , and  $\lambda_c = [L_x L_y + 2(L_y z_H) + 2(L_x z_H)] / D_x D_y$ . Although drawn as buildinglike, the element is generic, representing all obstacles relevant to airflow. Similarly, the concept is not limited to a grid array. It could include scattered trees, differently shaped houses, and winding streets that are more typical of real cities.

intermediate density. At the theoretical limit  $\lambda_p = 1.0$ , where the elements are so close they merge to form a new surface,  $z_0$  returns to its background value (i.e., the  $z_0$  used in the normalized scale is the *additional* roughness contributed by the tall elements). This behavior matches observations from wind tunnel studies with cylinders, cubes, and scale models of plant stands, and from field studies of vegetation (Raupach 1992). Further, it agrees with the wind tunnel work of Hussain and Lee (1980) who distinguish three flow regimes: *isolated flow*, in which elements are far apart and act as individual wake generators; *wake interference flow*, in which the spacing is close enough that the wakes reinforce each other; and *skimming flow*, in which the density of packing is so great that the main flow skips over the top of the elements. The intermediate flow regime is likely to generate the greatest roughness activity for the array.

Initially, as the density increases, the role of the original surface remains the dominant momentum sink. But at higher densities an increasingly large fraction of the total drag is exerted by the elements rather than the background, so the mean height of the momentum sink  $z_d$  starts to move upward; that is, there is a need to adjust the zero height datum. Wieringa (1993, p. 333) argues that this critical point occurs when the separated flow over the obstacles fails to reattach before having to react to the next obstacle, that is, near the transition between isolated and wake interference flows (Fig. 1). Beyond this point, the addition of elements continues to raise  $z_d$ . Eventually the packing becomes so dense that eddies have difficulty penetrating the interelement spaces (i.e., the “street” canyons) and the flow skims. Hence, the height of the “roofs” becomes the significant momentum sink and a new continuous surface datum is created (i.e.,  $z_H \sim z_d$  near  $\lambda_p = 1.0$ ). Unfortunately, there are no good observations of  $z_d$  that cover the full range of element densities (Raupach 1992), so it is difficult to verify this concept. Jackson (1981) gives a theoretical argument to support the idea that  $z_d/z_H$  versus  $\lambda_p$  has a 45° lower bound.

These arguments are unable to give the exact shape of the curves so they are only sketched as shaded zones in Fig. 1, but they are sufficient to suggest that it is reasonable to expect that methods to predict  $z_0$  and  $z_d$  should give estimates that track within them. Hereinafter these shaded areas are referred to as the “reasonable” zones or envelopes.

Other characteristics of the roughness geometry also may be significant in setting the aerodynamic properties of cities. The size and shape of the wake shed by a building depends on its width and depth (aspect ratio) as well as its height and distance to surrounding structures. Similarly, the buildings and trees are not randomly distributed. Often they are networked together, as in-line rows that follow the street pattern or as staggered arrays. Wind tunnel results suggest that  $z_0/z_H$  for a staggered array is about twice as large as it is for an equiv-

alent in-line array (Macdonald et al. 1999, manuscript submitted to *Atmos. Environ.*, hereinafter MHWG99). Further, flow normal to the street axis encounters greater roughness than when it is parallel (cf. trellised vineyards; Hicks 1973). Finally, an array of elements with similar heights is less rough than one with variable heights, even though the spatially averaged mean height may be the same. Hence, a measure of the height variance also is likely to be relevant (Rafailidis 1997; MHWG99). MHWG99 find that  $z_0/z_H$  increases approximately linearly with height variability for a given roughness density. The standard deviation of roughness element height is given by  $\sigma_H$ . With  $\lambda_p = 0.16$ ,  $z_0/z_H$  more than doubles if height variability  $\sigma_H/z_H$  is increased from 0% (all elements of equal height) to 50%; with  $\lambda_p = 0.44$ , the same increase in  $\sigma_H/z_H$  gives a sixfold increase in roughness.

Two simple criteria to judge methods to calculate  $z_d$  and  $z_0$  are that the estimates (1) do not exceed the mean height of the roughness elements  $\overline{z_H}$  and (2) follow the trend and lie within the broad confines of the shaded zones in Fig. 1. Ideally, a method should also incorporate the effects of element shape and street geometry in combination with the attack angle of the wind.

This paper is directed primarily toward estimation of  $z_d$  and  $z_0$  using morphometric methods, but it also provides predicted values for other aerodynamic properties of cities such as depth of the roughness sublayer and aerodynamic conductance (defined in section 3). As a by-product, the analysis generates the magnitudes of several geometric measures of urban morphometry that are of interest to urban climate studies in general (appendix A). Also presented is both a critical appraisal of existing field and wind tunnel studies and a database of the existing high-quality observations of  $z_d$  and  $z_0$  for real and scale model cities. The morphometric predictions are compared with these observed values. Based on the experience gained in this study, recommendations are made regarding the probable magnitude of the aerodynamic characteristics of cities and the best available methods to obtain new values.

## 2. Morphometric methods to determine zero-plane displacement and roughness lengths

The dependence of  $z_d$  and  $z_0$  on the size, shape, density, and distribution of surface elements has been studied using wind tunnels, analytical investigations, numerical modeling, and field observation (see reviews by Wieringa 1993; Bottema 1995a,b; 1997). The list of morphometric methods considered here is far from exhaustive; it includes those commonly used plus three recently developed methods (Raupach 1994; Bottema 1995a–c; Macdonald et al. 1998). Methods differ in terms of the attributes of the roughness elements and/or the weighting functions used.

In this section we outline the morphometric methods and their similarities and differences, and conduct a sen-

sitivity analysis of each. The dimensions used to characterize the surface geometry in the different methods are defined in Fig. 2. The methods are divided into three sets: a simple height-based “rule of thumb” and two sets distinguished by the type of aspect ratio (nondimensional area) used to describe the active surface presented to the flow. One set uses the fraction of the plan surface area covered by roughness elements ( $\lambda_p$ ), the other uses the frontal area index ( $\lambda_F$ ) of the elements as “seen” by the oncoming wind.

a. Methods

1) HEIGHT-BASED APPROACH

The most common morphometric approach is a simple rule of thumb (Rt), which holds that, to a first order,  $z_d$  and  $z_0$  are simply related to the height of the elements:

$$Rt_d \text{ is } z_d = f_d \overline{z_H} \quad (1)$$

and

$$Rt_0 \text{ is } z_0 = f_0 \overline{z_H}, \quad (2)$$

where  $f_d$  and  $f_0$  are empirical coefficients derived from observation. Garratt (1992) finds  $f_d \sim 0.67$  and  $f_0 \sim 0.10$  to be good overall mean values for land surfaces. Raupach et al. (1991) note that surveys of measured coefficients give  $f_d \sim 0.64$  and  $f_0 \sim 0.13$  for field crops and grass canopies and  $f_d \sim 0.8$  and  $f_0 \sim 0.06$  for forests. In their survey of urban dispersion parameterizations, Hanna and Chang (1992) suggest that  $f_d \sim 0.5$  and  $f_0 \sim 0.1$  are useful approximations. The latter value is a commonly quoted approximation for surfaces in general but no urban results were forwarded to support their choices. It could be hypothesized that, ceteris paribus, greater roughness will be generated by cities compared to forests because the drag coefficient for sharp-edged buildings is greater than for trees (Taylor 1988) and their porosity to airflow is essentially zero. On the other hand, these features may be compensated for by the lower density of elements in a city (see later). As a first expectation,  $f_d \sim 0.7$  and  $f_0 \sim 0.1$  are sketched in Fig. 1.

2) METHODS THAT USE HEIGHT AND PLAN AREAL FRACTION ( $\lambda_p$ )

Kutzbach (Ku) (1961) and Counihan (Co) (1971) used controlled arrays of roughness elements (Kutzbach outdoors on a frozen lake; Counihan in a wind tunnel) to derive  $f_d$  and  $f_0$  coefficients similar to those for Eqs. (1) and (2) but that also incorporate the plan areal fraction  $\lambda_p = A_p/A_T$  (Fig. 2). The equations proposed by both authors often are slightly misused. First, many workers use  $\lambda_p$  to specify the density of elements (e.g., Clarke et al. 1982; Rotach 1994), whereas Kutzbach’s original equation used the nondimensional ratio of the specific (ground) area to the lateral silhouette area of

the roughness elements ( $\lambda_F^{-1}$ ). It was only because of the specific dimensions of his elements (bushel baskets) that  $\lambda_p$  is coincidentally similar to  $\lambda_F$ . Second, power exponents different from those found by Kutzbach are often quoted: his original coefficients are 1.13 for  $z_0$  and 0.29 for  $z_d$  and his equations included an intercept term. Third, he considered his equations would only apply for  $\lambda_F \approx \lambda_p < 0.29$ :

$$Ku_d \text{ is } z_d = \lambda_x^{0.29} \overline{z_H} \quad \lambda_x \leq 0.29 \quad (3)$$

and

$$Ku_0 \text{ is } z_0 = \lambda_x^{1.13} \overline{z_H} \quad \lambda_x \leq 0.29. \quad (4)$$

Here we show the sensitivity of this method using both  $\lambda_F$  and  $\lambda_p$  (section 2b), but then use the equation based on  $\lambda_p$  because this has been the form most commonly used in the past.

Counihan, on the other hand, did not present a complete set of equations for all densities. He stated limits to the applicability of his equations but others have often extended them without comment (e.g., Clarke et al. 1982). Counihan defines

$$Co_0 \text{ as } z_0 = (1.08 \lambda_p - 0.08) \overline{z_H} \\ 0.1 < \lambda_p < 0.25. \quad (5)$$

In his paper, Counihan presents a curve that extends from  $\lambda_p = 0.0$  to 0.5. Using this curve, we have fitted the equation

$$Co_0 \text{ as } z_0 = \left( C_1 + \sum_{j=2}^{j=10} C_j \lambda_p^{j-1} \right) \overline{z_H}, \quad (6)$$

where  $C_1$  is 0.026 77,  $C_2$  is 1.3676,  $C_3$  is 15.98,  $C_4$  is 387.15,  $C_5$  is -4730,  $C_6$  is 32 057,  $C_7$  is -124 308,  $C_8$  is 27 162,  $C_9$  is -310 534, and  $C_{10}$  is 14 444. While the number of coefficients may appear excessive, it is necessary to retain them to describe the curve adequately. He also presents a curve for  $z_d$ , which can be described by

$$Co_d \text{ as } z_d = [(1.4352 \lambda_p) - 0.0463] \overline{z_H}. \quad (7)$$

Equations (6) and (7) are used in this study.

Using similar variables, Kondo and Yamazawa (1986) developed a method (Ko) to determine  $z_0$  for Japanese cities. It uses areal extent of the individual roughness elements and their heights ( $z_{H_i}$ ), weighted by a constant factor, 0.25:

$$Ko_0 \text{ is } z_0 = 0.25 \frac{\sum_{i=1}^n z_{H_i} A_{P_i}}{A_T}. \quad (8)$$

Note that Kondo and Yamazawa (1986) do not incorporate  $z_d$  in their log-law equation. They compare their data to Yamamoto and Shimanuki (1964) after modification to include  $z_d$ .

Bottema (1995b) presents a method (Ba) explicitly intended for use in urban areas for situations where the

airflow is not perpendicular to the buildings. It is a simplification of the more complex approach discussed in the following section (Bottema 1995c, 1997). It requires information on height and area of the roughness elements:

$$\text{Ba}_d \text{ is } z_d = \left[ \frac{\sum A_{pb} + \sum (1 - p)A_{pt}}{A_T} \right]^{0.6} \bar{z}_H \quad (9)$$

and  $\text{Ba}_0$  is

$$z_0 = (\bar{z}_H - z_d) \times \exp \left[ - \frac{0.4}{\left( 0.5 \frac{\sum C_{db} L_{yib} z_{Hib} + \sum C_{dt} L_{yit} z_{Hit}}{A_T} \right)^{0.5}} \right] \bar{z}_H \quad (10)$$

where the subscript *b* refers to buildings, *t* refers to trees, and *p* is a coefficient to allow for the porosity of trees. Bottema (1995b) assigns a value of 0.8 to  $C_{db}$  (the drag coefficient for buildings), and  $C_{dt}$  (the drag coefficient for trees) is set equal to  $C_{db}(1 - p)$ . The horizontal dimensions of the roughness elements are denoted by *L*.

### 3) METHODS THAT CONSIDER HEIGHT AND FRONTAL AREA INDEX ( $\lambda_F$ )

The frontal area index (which combines mean height, breadth, and density of the roughness elements) is defined (Raupach 1992) as

$$\lambda_F = \bar{L}_y \bar{z}_H \rho_{el} = \bar{L}_y \bar{z}_H / (\bar{D}_x \bar{D}_y), \quad (11)$$

where  $\bar{L}_y$  is the mean breadth of the roughness elements perpendicular to the wind direction;  $\rho_{el}$  is the density [number (*n*) of roughness elements per unit area ( $\rho_{el} = n/A_T$ )];  $\bar{D}_x$  is the average interelement spacing (between element centroids), in the alongwind direction; and  $\bar{D}_y$  is the average in the crosswind direction (Fig. 2). Typical values of frontal area index are in the range 0.1–0.25 for crops and about 1–10 for forests (Raupach et al. 1991).

Lettau (1969) used the observations of Kutzbach to develop a formula (Le) for irregular arrays of reasonably homogenous elements:

$$\text{Le}_0 \text{ is } z_0 = 0.5 \bar{z}_H \lambda_F. \quad (12)$$

Lettau did not specify limits for his formula; however, it is widely recognized that it fails when roughness area density  $\lambda_p$  or  $\lambda_F$  increases beyond 0.2–0.3 (see discussion in Macdonald et al. 1998). Lettau's formula is often quoted in relation to urban roughness estimates and has been implemented for whole cities using detailed morphometric inventories, for example, Baltimore, Maryland (Nicholas and Lewis 1980), and Ogaki City, Japan (Takahashi et al. 1981).

Recognizing the limitations of the Le model at higher

roughness densities and that it does not give values for  $z_d$ , Macdonald et al. (1998) present a new derivation that starts from fundamental principles and some simple assumptions. This method (Ma) yields values of  $z_d$  and  $z_0$ , and the latter decline at higher densities beyond a single peak:

$$\text{Ma}_d \text{ is } \frac{z_d}{z_H} = 1 + \alpha^{-\lambda_p} (\lambda_p - 1) \quad (13)$$

and  $\text{Ma}_0$  is

$$\frac{z_0}{z_H} = \left( 1 - \frac{z_d}{z_H} \right) \exp \left\{ - \left[ 0.5 \beta \frac{C_D}{k^2} \left( 1 - \frac{z_d}{z_H} \right) \lambda_F \right]^{-0.5} \right\}, \quad (14)$$

where  $\alpha$  is an empirical coefficient,  $C_D$  is a drag coefficient (1.2), *k* is von Kármán's constant, and  $\beta$  is a correction factor for the drag coefficient (the net correction for several variables, including velocity profile shape, incident turbulence intensity, turbulence length scale, and incident wind angle, and for rounded corners). The two empirical coefficients ( $\alpha$  and  $\beta$ ) have to be set a priori. Macdonald et al. (1998) provide a graphical sensitivity analysis that demonstrates responses to changes in these values. They “calibrate” their equations using wind tunnel data and recommend that for staggered arrays of cubes  $\alpha = 4.43$  and  $\beta = 1.0$ . These coefficients are the values used here.

Raupach (1994) used his previous analytic treatment of drag and drag partition on rough surfaces (Raupach 1992) to derive expressions for  $z_d$  and  $z_0$  as a function of height and frontal area index (Raupach 1994, 1995):

$$\text{Ra}_d \text{ is } \frac{z_d}{z_H} = 1 + \left\{ \frac{\exp[-(c_{d1} 2\lambda_F)^{0.5} - 1]}{(c_{d1} 2\lambda_F)^{0.5}} \right\} \quad (15)$$

and

$$\text{Ra}_0 \text{ is } \frac{z_0}{z_H} = \left( 1 - \frac{z_d}{z_H} \right) \exp \left( -k \frac{U}{u_*} + \psi_h \right), \quad (16)$$

where

$$\frac{u_*}{U} = \min \left[ (c_s + c_R \lambda_F)^{0.5}, \left( \frac{u_*}{U} \right)_{\max} \right] \quad (17)$$

and  $\psi_h$  is the roughness sublayer influence function, *U* and  $u_*$  are the large-scale wind speed and the friction velocity;  $c_s$  and  $c_R$  are drag coefficients for the substrate surface at height  $z_H$  in the absence of roughness elements, and of an isolated roughness element mounted on the surface, respectively; and  $c_{d1}$  is a free parameter. The values specified by Raupach (1994) are  $c_s = 0.003$ ,  $c_R = 0.3$ ,  $(u_*/U)_{\max} = 0.3$ ,  $\psi_h = 0.193$ , and  $c_{d1} = 7.5$ . Raupach discusses the errors likely to be associated with these values and Bottema (1995b) considers their appropriateness in urban studies.

Raupach et al. (1991) note that complete specification of the roughness is likely to require other aspect ratios in addition to  $\lambda_F$ . Bottema (1995c, 1997) proposed a

TABLE 1. Equations for  $z_d$  using the Bottema (1995c) method ( $Bo_d$ ). See Fig. 2 and text for additional definition of symbols.

Normal:	Low densities	High densities ( $W_x < L_{ca} + L_{bo}$ )*
$z_d = (L_y/D_y)z_{dpl}$	$\frac{z_{dpl}}{z_H} = \frac{L_x + 0.33(L_{ca} + L_{bo})}{D_x}$	$\frac{z_{dpl}}{z_H} = \frac{L_x + 0.33\left(2 - \frac{W_x}{L_{ca} + L_{bo}}\right)W_x}{D_x}$
Staggered ( $W_y/L_y > 1$ ):	Low densities	High densities ( $W_x + D_x < L_{ca} + L_{bo}$ )
$z_d = 2(L_y/D_y)z_{dpl}$	$\frac{z_{dpl}}{z_H} = \frac{L_x + 0.33(L_{ca} + L_{bo})}{2D_x}$	$\frac{z_{dpl}}{z_H} = \frac{L_x + 0.33\left(2 - \frac{W_x + D_x}{L_{ca} + L_{bo}}\right)(W_x + D_x)}{2D_x}$
Dense, staggered ( $W_y/L_y < 1$ ):	$z_d = z_{dpl} = \left(\frac{W_y}{L_y}\right) \left[ \frac{L_x + 0.33\left(2 - \frac{W_x + D_x}{L_{ca} + L_{bo}}\right)(W_x + D_x)}{2D_x} \overline{z_H} \right] + \left(1 - \frac{W_y}{L_y}\right) \left[ \frac{L_x + 0.33\left(2 - \frac{W_x}{L_{ca} + L_{bo}}\right)W_x}{D_x} \overline{z_H} \right]$	

\*  $L_{ca} + L_{bo} = 4[L_y \overline{z_H} / (0.5L_y + z_H)]$ , where  $L_{ca}$  is the length of the frontal vortex and  $L_{bo}$  is the length of the recirculation zone.

model (Bo) explicitly for the urban environment that incorporates extra measures of the elements ( $D_x, D_y, L_x, L_y, W_x$ , and  $W_y$ ; for definitions see Fig. 2):

$$Bo_0 \text{ is } \frac{z_0}{z_H} = \frac{\overline{z_H} - z_{dpl}}{\overline{z_H}} \exp\left[-\frac{k}{(0.5\lambda_F C_{dh})^{0.5}}\right], \quad (18)$$

where  $z_{dpl}$  is a (in-plane sheltering) displacement height calculated based on the density and pattern of the building arrangement (normal or staggered) (see Table 1), and  $C_{dh} = 1.2 \max[1 - 0.15(L_x/z_H), 0.82] \min[0.65 + 0.06(L_y/z_H), 1.0]$ . Bottema recommends use of the equations for staggered building arrangements when flow is oblique to the roughness elements.

*b. Sensitivity analysis of morphometric methods*

The sensitivity of each of the morphometric methods to changes in the dimensions and spacing of the roughness elements is given in Fig. 3. In all cases the roughness parameters are normalized by  $z_H$ . A wider range of analyses could have been reported; however, only physically realistic combinations of element dimensions are presented, and results are truncated if the method has applicability limits (e.g., Ku and Co). Although the rule of thumb does not vary with density, it is included here (using the coefficients  $f_d = 0.7$  and  $f_0 = 0.1$ ) because it is often quoted as a first-order guide. The sensitivity analysis was conducted with building dimensions ( $\overline{z_H} = 5$  m) and total area held fixed. In each run the number of buildings per unit area was increased (thus increasing the density and decreasing the space around each building). Some methods required lateral dimensions to be defined. In run 1,  $L_x$  and  $L_y$  were set to 5 m. In run 2, the buildings were kept square but increased in size ( $L_y = L_x = 14.4$  m). In run 3, rectangular buildings were considered with  $L_x = 10.0$  m and  $L_y = 20$  m ( $2L_x$ ). The total area of the buildings ( $L_x L_y$ ) in runs 2 and 3 was the same.

The  $z_d/z_H$  results (Figs. 3a,b) show that all methods except  $Rt_d$  give values that increase with roughness density across the range of densities considered here. The  $Ra_d$  estimates asymptotically approach those of  $Rt_d$ . The  $Ra_d$  estimates do not show differences if areal extent of roughness ( $\lambda_p$ ) or building shape ( $L_x:L_y$ ) is varied. On the other hand,  $Bo_d$  values are very sensitive to element shape. Unlike the other methods, Bo is dependent on dimensions in addition to  $\lambda_p$  and  $\lambda_F$  (see model equations). For  $z_d/z_H$  the Ba model collapses onto one function. At low  $\lambda_p$ , Ma is very similar to Ba, but is greater when  $\lambda_p > 0.2$ . For run 1 of Bo,  $z_d/z_H$  becomes unity at intermediate values of  $\lambda_F$ , but for runs 2 and 3 it reaches unity at what appear to be low values of density. This result arises because  $\lambda_p = \lambda_F(L_x/z_H)$ , so  $\lambda_p = 1.0$  is reached at smaller  $\lambda_F$  values, that is, 0.24 and 0.5, respectively. With this possible exception, none of the methods give unreasonable estimates of  $z_d/z_H$ , at least based on the heuristic arguments presented earlier, although the Raupach method yields rather low values at very high densities.

Of the  $z_0/z_H$  methods, five show the required form with a peak at intermediate densities ( $Ba_0, Co_0, Ra_0, Ma_0$ , and  $Bo_0$ ), although the magnitude of the peak varies from about 0.04 to 0.28, and its position on the density scale ranges from about 0.28 to 0.5 for  $\lambda_p$  methods and from about 0.07 to 0.3 for those using  $\lambda_F$  (Figs. 3c,d). The  $Ma_0$  method yields results very similar to those of  $Bo_0$  although the peaks tend to be lower and occur at smaller  $\lambda_F$ . Here  $Ra_0$  asymptotically approaches  $Rt_0$ . For  $z_0/z_H$ , the relative behavior of both Bottema models is the same, at least using the changes in building size and area considered here. Increasing the size of the roughness elements while holding the shape of the buildings (square) constant (runs 1 and 2) results in a decrease in  $z_0/z_H$ ; changing the relative dimensions of the roughness elements from square to rectangular, while holding building area constant (runs 2 and 3) increases  $z_0/z_H$ . Because of their dependence on param-

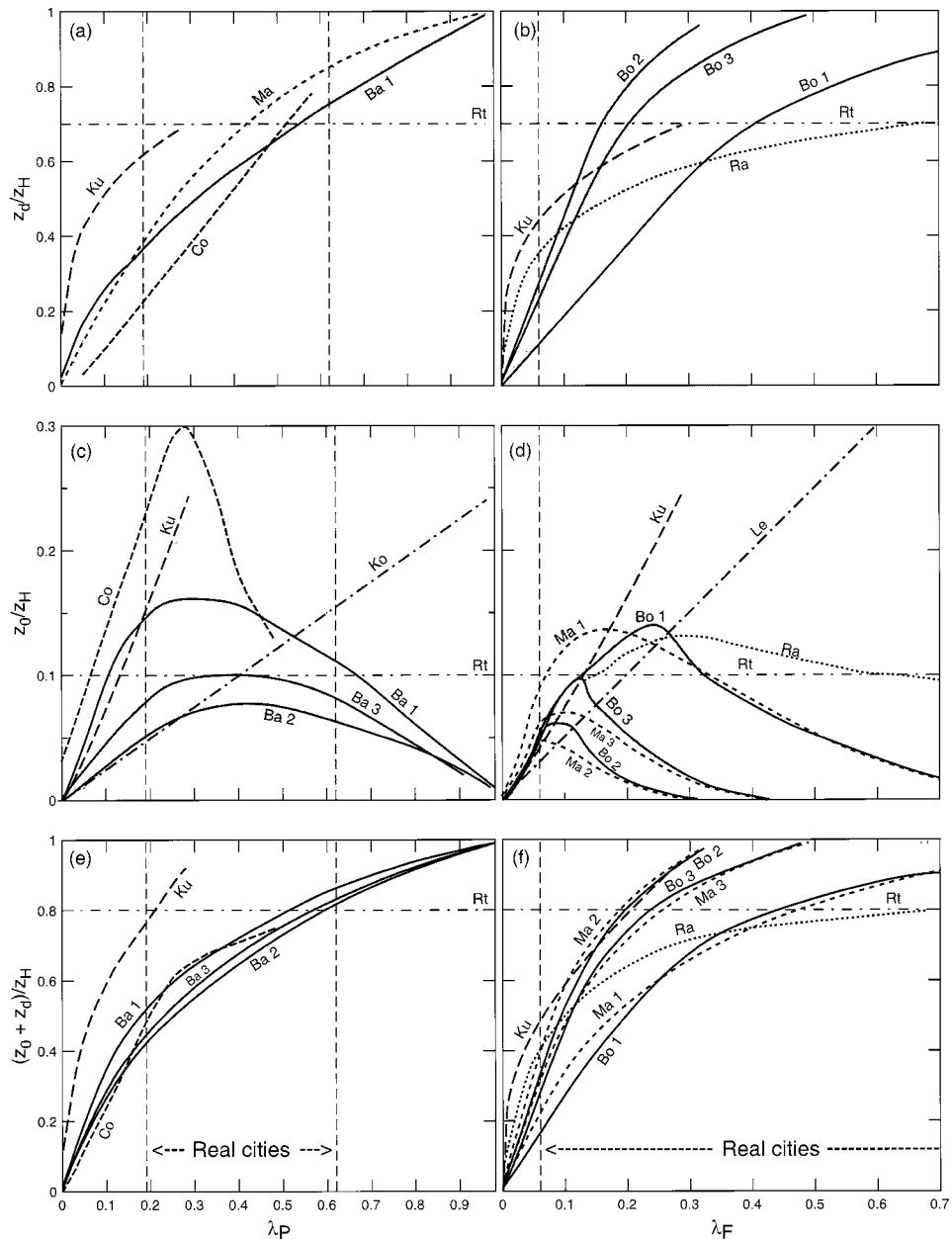


FIG. 3. Sensitivity analysis of morphometric methods to determine  $z_d$  and  $z_0$  normalized with respect to mean element height  $z_H$ . Normalized length  $z_d/z_H$  as a function of (a)  $\lambda_P$  determined using the  $Ba_d$ ,  $Co_d$ ,  $Ku_d$ , and  $Ma_d$  methods; and (b)  $\lambda_F$  for  $Bo_d$ ,  $Ku_d$ , and  $Ra_d$ . Normalized length  $z_0/z_H$  as a function of (c)  $\lambda_P$  for the  $Ba_0$ ,  $Co_0$ ,  $Ko_0$ , and  $Ku_0$  methods; and (d)  $\lambda_F$  for  $Bo_0$ ,  $Ku_0$ ,  $Le_0$ ,  $Ma_0$ , and  $Ra_0$ . Normalized length  $(z_0 + z_d)/z_H$  as a function of (e)  $\lambda_P$  for  $Ba_{d,0}$ ,  $Co_{d,0}$ , and  $Ku_{d,0}$ ; and (f)  $\lambda_F$  for the  $Bo_{d,0}$ ,  $Ku_{d,0}$ ,  $Ma_{d,0}$ , and  $Ra_{d,0}$  methods. Methods with three values incorporate the following sets of dimensions: run 1,  $L_x = 5$  m,  $L_y = L_x$ ; run 2,  $L_x = 14.14$  m,  $L_y = L_x$ ; run 3,  $L_x = 10$  m,  $L_y = 2 L_x$ . The rule-of-thumb coefficients are  $Rt_d = 0.7$ ,  $Rt_0 = 0.1$ , and  $Rt_{d,0} = 0.8$ . Vertical dashed lines define the range of real urban roughness densities, and shading defines the reasonable zones (both explained in relation to Fig. 1).

eters beyond  $\lambda_P$  or  $\lambda_F$  alone, the Bo, Ba, and Ma methods, unlike the other models, do not collapse onto a single function, and these methods are very sensitive to changes in the dimensions of the roughness elements.

For  $\lambda_P < 0.6$  and  $\lambda_F < 0.4$  most methods give magnitudes of  $z_0/z_H$  that lie within the reasonable zone (Fig.

1). The exceptions are the rather large peak predicted by  $Co_0$  and the small values obtained in run 2 for both  $Bo_0$  and  $Ma_0$ . At greater densities,  $Ko_0$  and  $Le_0$  unrealistically predict that  $z_0/z_H$  continues to increase as the elements are packed more closely. These two methods may have some utility in the low to medium range of

real-world densities but not across the full range—a conclusion also reached in earlier studies. Kutzbach’s method ( $Ku_0$ ) particularly is limited because its applicability covers only a small part of the range of densities found in real cities.

In applications, such as wind profile analysis, it is the sum ( $z_0 + z_d$ ) that is required, so this quantity is given in Figs. 3e,f for those methods that calculate both parameters. All values take on a shape dominated by  $z_d$ , which should caution users not to overlook the inclusion of  $z_d$  and take care in its estimation. Since use of  $Ku$  is limited to small densities, and even then  $(z_0 + z_d)/z_H$  approaches unity, it lacks promise. All other methods produce an appropriate general form, but, at any given density, estimates differ widely. Overall it appears that the Ba, Bo, Ma, and Ra schemes show reasonable correspondence with intuition (Fig. 1). The Bo method predicts considerable sensitivity to roughness element shape and/or wind direction characteristics. The Ra and Ma schemes could be made more sensitive if the coefficients [section 2a(3)] were allowed to vary.

The methods  $Rt_0$  and  $Rt_d$  cannot predict changes in response to different roughness densities. Nevertheless, these best-fit simplifications may still have some utility for back-of-the-envelope-type work. This suitability arises because of the probable form of the relations between  $z_d/z_H$  and  $z_0/z_H$  and roughness density within the range of real-world urban densities (Figs. 1, 3). In particular, the expected form of  $z_0/z_H$ , with a peak at intermediate densities, means that, while a constant ratio may overpredict at the low and high ends and underpredict at the peak, across the range it does not yield unreasonable values.

Overall these results indicate that a relatively large range of roughness parameter values can result from use of morphometric approaches, but, when measured against the crude requirements set out at the start of this paper, most methods have merit. However, given the number of variables involved and their complex interdependence, we cannot be sure of the real-world significance of any differences between methods suggested by this type of sensitivity analysis.

In the following sections we define two other aerodynamic characteristics of cities, and give methods to calculate them from morphometric data; then the full set of morphometric methods is applied to real-world configurations of urban roughness elements using the observed characteristics of sites in seven North American cities.

### 3. Other aerodynamic characteristics

#### a. Blending height ( $z_r$ )

Each roughness element distorts the flow and increases turbulence in its wake. The primary roughness elements in a city are buildings and trees, but aerodynamically they behave very differently. Buildings are sharp-

edged bluff bodies that cause flow separation and strong vortex shedding, whereas trees are porous and somewhat pliant. The flow in the vicinity of these objects and immediately above them in what is called the roughness sublayer is three-dimensional, comprises many scales, and is almost chaotic. At the top of the roughness sublayer, turbulent mixing smears individual wakes sufficiently to cause the flow to become independent of horizontal position. This height, termed the blending height  $z_r$ , represents the minimum elevation above a city at which observations are representative of the integrated surface rather than of its individual elements. The magnitude of  $z_r$  is thought to depend on the height and spatial arrangement of the elements (for a review see Raupach et al. 1991; Claussen 1995).

Here we use four measures of  $z_r$ . Two, attributable to Pasquill (1974) and Garratt (1978), are based on the height of the elements alone:

$$Pa_r, Ga_r \text{ are } z_r = f_r \overline{z_H}, \quad (19)$$

where  $f_r$  is an empirical coefficient with values of 2.5 and 4.5 as suggested by Pasquill and Garratt, respectively. Pasquill’s value expresses the common rule of thumb that an obstacle’s effect on the flow extends to about  $1.5z_H$  above its own height. Garratt’s coefficient is based on the results of flux measurements above a savanna forest.

On the basis of wind tunnel experiments over roughness arrays, Mulhearn and Finnigan (1978) suggest that a more relevant measure governing the blending height is the interelement spacing, such that

$$Mu_r \text{ is } z_r = 2\overline{D_x}, \quad (20)$$

Raupach et al. (1980) combine the ideas of height and spacing from a wind tunnel study, giving

$$Ra_r \text{ is } z_r = \overline{z_H} + 1.5(\overline{D_x} - \overline{L_x}). \quad (21)$$

Other equations have been forwarded but they require  $z_0$  and/or  $z_d$  as input (see, e.g., Garratt 1980; Raupach and Legg 1984; Fazu and Schwerdtfeger 1989; Claussen 1995). Since the aim of this study is to evaluate ways to find  $z_0$  and  $z_d$ , to avoid circular reasoning these methods are not considered further.

#### b. Surface conductance ( $g_{aM}$ )

In neutral stability the turbulent flux of horizontal momentum ( $\tau_0$ ) can be related to the mean flow in the surface layer using a bulk aerodynamic conductance  $g_{aM}$  or a neutral drag coefficient  $C_D$ , both of which depend on surface aerodynamic properties:

$$g_{aM} = \tau_0/\rho_a u = k^2 u \{\ln[(z_s - z_d)/z_0]\}^{-2} = C_D u, \quad (22)$$

where  $\rho_a$  is the density of air and  $u$  is the wind speed. In order to standardize values and to be above the blending height, we set  $u = 5 \text{ m s}^{-1}$  at a reference height of  $3z_H - z_d$ . The surface conductance is an important parameter in the Combination Model for evaporation used

by Grimmond and Oke (1991) to calculate urban evaporation, and is part of the deposition velocity that characterizes the transport of inert pollutants to urban surfaces (Hicks and Hosker 1987).

**4. Application of morphometric methods to North American cities**

*a. Geographic Information Systems (GISs)*

The geometric methods outlined above were applied to neighborhoods in seven North American cities where other urban meteorological measurements have been conducted (Grimmond and Oke 1995, 1998). In Table 2 each site is identified by a one- or two-letter location code and the year in which the measurements were conducted (“w” is added to the 1992 Chicago site name to indicate that the site considered here is centered on the wind profile tower and not the flux tower referred to in other of our papers). The sites are sorted in increasing order by average roughness element height, based on  $\lambda_F$  (see appendix A).

The study areas represent a range of building styles and spatial arrangements. Five of the sites are characterized by detached one- to two-story houses surrounded by vegetation (trees, shrubs, and grass). One site is a light industrial area in Vancouver (V192) with one- and two-story warehouse- and light industrial-type structures (for a photograph see Fig. 8f). The last two are central city sites: one is in the old colonial core of Mexico City (Me93) with four- and five-story institutional buildings; the other is in Vancouver (Vd92) with a mix of multistory towers that rise above two- to five-story blocks of office and commercial buildings (see photograph in Fig. 8k). Suburban residential sites dominate the database because this land use category occupies by far the largest area in most North American cities; thus, the findings have wide applicability. Moreover, such sites are relatively easy to find, have relatively homogeneous structure, and often possess relatively good fetch.

For each site, a GIS has been developed from aerial photographs and field surveys. Following procedures described by Grimmond and Souch (1994), areas of similar morphology and surface materials were delimited on aerial photographs. Representative information on the density of buildings and trees and the percent cover of different surface types was obtained by sampling randomly within each of the mapped units. Field observations at randomly chosen locations provided checks on the density and percent cover data and more detailed information on the characteristics of the built and vegetative materials and the three-dimensional nature of the urban surface.

In this study, the height, breadth, areal extent, and density of roughness elements are restricted to those of buildings, trees, and large shrubs. Smaller obstacles (e.g., traffic signs, fences, utility poles, other garden

TABLE 2. Location of study sites, the mean and standard deviation of the height of their roughness elements (buildings  $\bar{z}_{hb}$ , trees  $\bar{z}_{ht}$ , averaged based on plan area,  $\bar{z}_{HAP}$ , and averaged based on frontal area,  $\bar{z}_{FAF}$ ), and mean nondimensional surface area ratios (plan  $\lambda_p$ , frontal  $\lambda_F$ , complete  $\lambda_C$ , and aspect  $\lambda_S$ ) for the surroundings of the tower (variance shown in Fig. A1). Ordered downward by increasing  $\bar{z}_{HAP}$ ; UTZ, urban terrain zones based on the structural classification of Ellefsen (1990–91).

Site	Code	UTZ	Latitude, longitude	$\bar{z}_{FAF}$ (m)	$\bar{z}_{hb}$ (m)	$\bar{z}_{ht}$ (m)	$\bar{z}_{HAP}$ (m)	$\lambda_p$	$\lambda_F$	$\lambda_C$	$\lambda_S$
<b>Suburban residential</b>											
Tucson, AZ	T90	Do3	32°07'N, 110°56'W	5.1 ± 0.8	5.2 ± 0.8	4.1 ± 0.2	4.8 ± 0.8	0.33	0.19	1.45	0.54
Sacramento, CA	S91	Do3	38°39'N, 121°30'W	6.0 ± 0.5	4.8 ± 0.2	6.7 ± 0.5	5.1 ± 0.3	0.58	0.23	1.63	1.21
San Gabriel, CA	Sg94	Do3	34°05'N, 118°05'W	6.2 ± 0.3	4.7 ± 0.2	7.3 ± 0.3	5.3 ± 0.2	0.36	0.14	1.31	0.43
<b>Light industrial</b>											
Vancouver, BC, Canada	V192	Do4	49°16'N, 123°06'W	6.7 ± 0.1	5.8 ± 0.1	8.6 ± 0.2	6.0 ± 0.2	0.46	0.13	1.39	0.57
<b>Suburban residential</b>											
Chicago, IL	C92w	Dc3	41°57'N, 87°48'W	7.8 ± 0.4	6.7 ± 0.5	9.6 ± 1.1	7.1 ± 0.4	0.47	0.21	1.51	0.97
Miami, FL	Mi95	Do3	25°44'N, 80°22'W	7.9 ± 1.2	8.0 ± 2.1	8.5 ± 0.2	7.5 ± 1.5	0.35	0.16	1.37	1.03
Vancouver, BC, Canada	Vs92	Dc3	49°15'N, 123°04'W	8.4 ± 0.6	4.7 ± 0.2	14.0 ± 0.1	6.1 ± 0.3	0.43	0.19	1.65	0.90
Chicago, IL	C95	Dc3	41°57'N, 87°48'W	9.5 ± 1.7	5.9 ± 1.3	11.7 ± 1.0	8.3 ± 0.9	0.38	0.28	1.74	1.07
Arcadia, CA	A94	Do3	34°08'N, 118°03'W	12.0 ± 1.0	5.2 ± 0.3	14.1 ± 0.5	8.9 ± 0.9	0.53	0.33	1.78	1.19
<b>Central city</b>											
Mexico City, Mexico	Me93	A2	19°26'N, 99°08'W	19.1 ± 5.8	18.4 ± 6.6	21.8 ± 7.8	17.7 ± 4.4	0.47	0.19	1.73	1.19
Vancouver, BC, Canada	Vd92	Dc1	49°16'N, 123°45'W	34.3	34.3	34.3	34.3	0.39	0.30	2.20	1.40

plants, ground unevenness, etc.) are neglected. This restriction gives a bias toward underestimation of roughness properties. Following Bottema (1995b), the porosity  $p$  of the trees is considered by adjusting their dimensions by the factor  $(1 - p)$ . When deciduous trees are in leaf,  $p$  is set to 0.2, and, after leaf fall, it is set to 0.6 (Heisler 1984; Heisler and DeWalle 1988).

Models that use  $\lambda_F$  explicitly require information about the orientation of the roughness elements in order to determine the breadth of the elements relative to the airflow [Eq. (11)]. Width is determined initially from

$$\bar{L}_y = \left[ \frac{(A_p/A_T)(1/\rho_{cl})}{L_x/L_y} \right]^{0.5} L_x/L_y, \quad (23)$$

and wind direction ( $\varphi$ ) together with the mean length and width is used to determine the mean horizontal element dimension  $\tilde{L}$ :

$$\tilde{L} = \bar{L}_y \cos\varphi + \bar{L}_x \sin\varphi. \quad (24)$$

*b. Source areas*

Since a city displays spatial variability in its surface (including aerodynamic) character, estimates of wind profile parameters vary with direction around a site. Therefore, it is necessary to identify which portion of the upstream surface contributes to the aerodynamic character at a given measurement site and height.

The location and dimensions of these upstream patches, termed source areas, were obtained using the Flux Source Area Model (FSAM) of Schmid (1994). FSAM gives a source area strength for each grid square (in this case  $5 \text{ m} \times 5 \text{ m}$  pixels) in the spatial domain. Source areas were calculated for each site using the same non-dimensional height ( $z_{\text{ref}}/z_0 = 33$ ), near-neutral stability ( $z_{\text{ref}}/L' = -0.04$ , where  $L'$  is the Obukhov length), and a lateral turbulence parameter  $\sigma_v/u_* = 1.9$ . The difference between the sensor height and  $z_d$  is the reference height  $z_{\text{ref}}$ , and  $\sigma_v$  is the horizontal crosswind standard deviation of the wind speed fluctuations. Source areas contributing 90% of the flux concentration were used in the calculations.

*c. GIS database sampling and averaging*

For each site, the GIS database was sampled, using the source weight filter output from FSAM, 24 times at  $15^\circ$  intervals (sectors). The centerline for sector 1 is  $15^\circ$ , for sector 2 it is  $30^\circ$ , etc. At all sites the same weighting filter was used to sample the database (spatial resolution  $5 \text{ m} \times 5 \text{ m}$ ). For a site, the mean value of the dimensions of a property (height, breadth, etc.) is the average of the values for the 24 complete source areas. The effective aerodynamic parameters ( $z_d$ ,  $z_0$ , and  $g_{aM}$ ) (Taylor 1987) for the individual source areas (sectors) are determined by

$$(\ln z_0^{\text{eff}}) = \sum_{i=1}^n [\ln(z_{0i})w_i], \quad (25)$$

where  $w_i$  is the weighting for the source area strength. In contrast,  $z_r$  is based on the mean characteristic of the sites, including  $z_{H_i}$ :

$$z_{H_i} = \sum w_i z_{H_i}. \quad (26)$$

Because FSAM-weighted values are used, the numbers calculated may be different than nonweighted means for these sites reported elsewhere.

**5. Morphometric predictions of aerodynamic characteristics of cities**

Results calculated for the individual sectors by the methods in section 2 are presented in Fig. 4. All values presented include both buildings and trees. The data are presented in a way that allows consideration of the range of values determined by each method, the variability among sectors in a given city, and the differences among cities due to their unique surface forms.

*a. Zero-plane displacement length ( $z_d$ )*

Values of  $z_d$  from the morphometric methods at the residential and industrial sites typically lie in the range 2–5 m; at the city center in Mexico City  $z_d$  is about 10 m, and in downtown Vancouver it is about 19 m (Fig. 4a). In cities and at sites with relatively small  $\bar{z}_H$  (typically on the left side of Fig. 4) the range of  $z_d$  values given by the different methods also is relatively small. For the residential sites, the least variability is found at Vs92 and S91. The relation between variability and roughness height may be real or simply may be an artifact of the inclusion of height in all formulas. At sites with lower  $\bar{z}_H$ ,  $Rt_d$  estimates tend to be the largest, but this bias is lost as the mean height increases. The Ku method consistently fails to yield results because of the constraints of the model [Eq. (3)]. There are also many cases when Co cannot be used because  $\lambda_p$  lies outside the range of applicability; the most notable is S91. When normalized by  $\bar{z}_H$ , the results can be compared with the bounds of reasonableness outlined on Fig. 1, and it is possible to make some general assessment of the promise of each method. Given the respective weighting schemes used to calculate the aerodynamic parameters and the average characteristics of the sites [Eqs. (25), (26)], the predictions do not collapse onto simple relations with  $\lambda_p$  or  $\lambda_F$  (Fig. 5). (Note that only Ba, Bo, Co, Ma, Ra, and Rt are shown.) Simple visual inspection suggests that most methods perform acceptably; that is, estimates follow the trend of the suggested central curve and most values lie within the expected zone. Interestingly, while Ba and Ma produce similar results in the sensitivity analyses, their application to real-world data yields quite different results for each method (Fig. 5) because of the different surface parameters they incor-

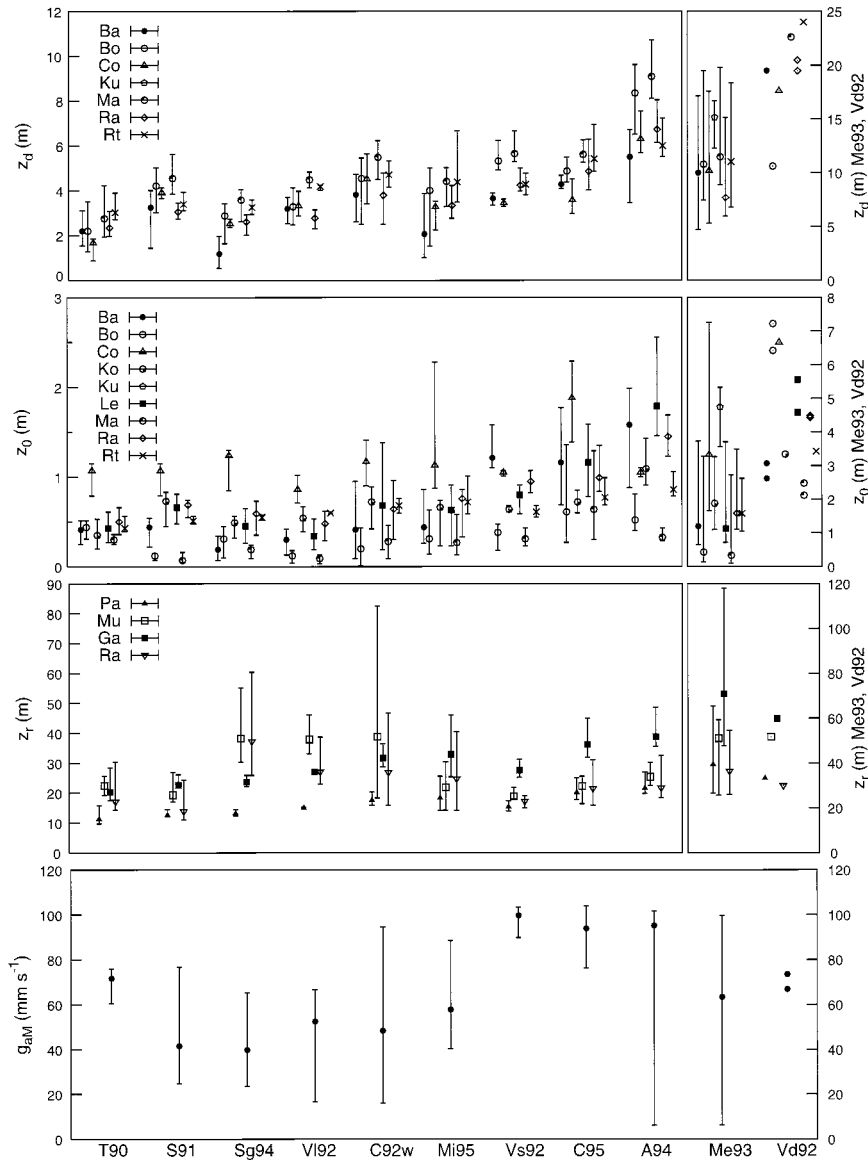


FIG. 4. Aerodynamic characteristics  $z_d$ ,  $z_0$ ,  $z_r$ , and  $g_{aM}$  of the urban sites listed in Table 2, calculated using the morphometric methods indicated in the key in the top left of each panel. Note the separate scales at right for Me93 and Vd92 in the top three panels. Median (dot) and maximum and minimum (bars) values are shown. Sites (along bottom) are ordered from left to right by increasing  $z_r$ .

porate. Here Ku suffers from its restricted range of applicability, thereby yielding few estimates. When compared visually, Bo, Ra, Ma, and Co perform best. Here Ba also follows the pattern, but a more significant fraction of its outliers are below the suggested zone. As in Fig. 3, the trend of the Ra results shows slightly lesser sensitivity to roughness density, so at larger  $\lambda_F$  its estimates are somewhat low. In the range of densities represented in these North American cities, Rt with  $f_d = 0.7$  generates  $z_d$  values that are within the bounds of reasonable values, but at lower densities Rt yields estimates that are likely to be too large.

*b. Surface roughness length ( $z_0$ )*

Surface roughness lengths for the residential and industrial sites, as predicted by morphometric methods, typically lie in the range 0.2–1.3 m (Fig. 4b); only the sites with many tall trees (C95, A94) have values above 1 m. The value for central Mexico City varies among methods with a median of about 1.7 m. In central Vancouver it is hard to assess, given the spread from about 2 to 7 m. As was found with  $z_d$ , the absolute sectoral variability is related to the mean height of the elements. All sites yield relatively closely clustered estimates, ex-

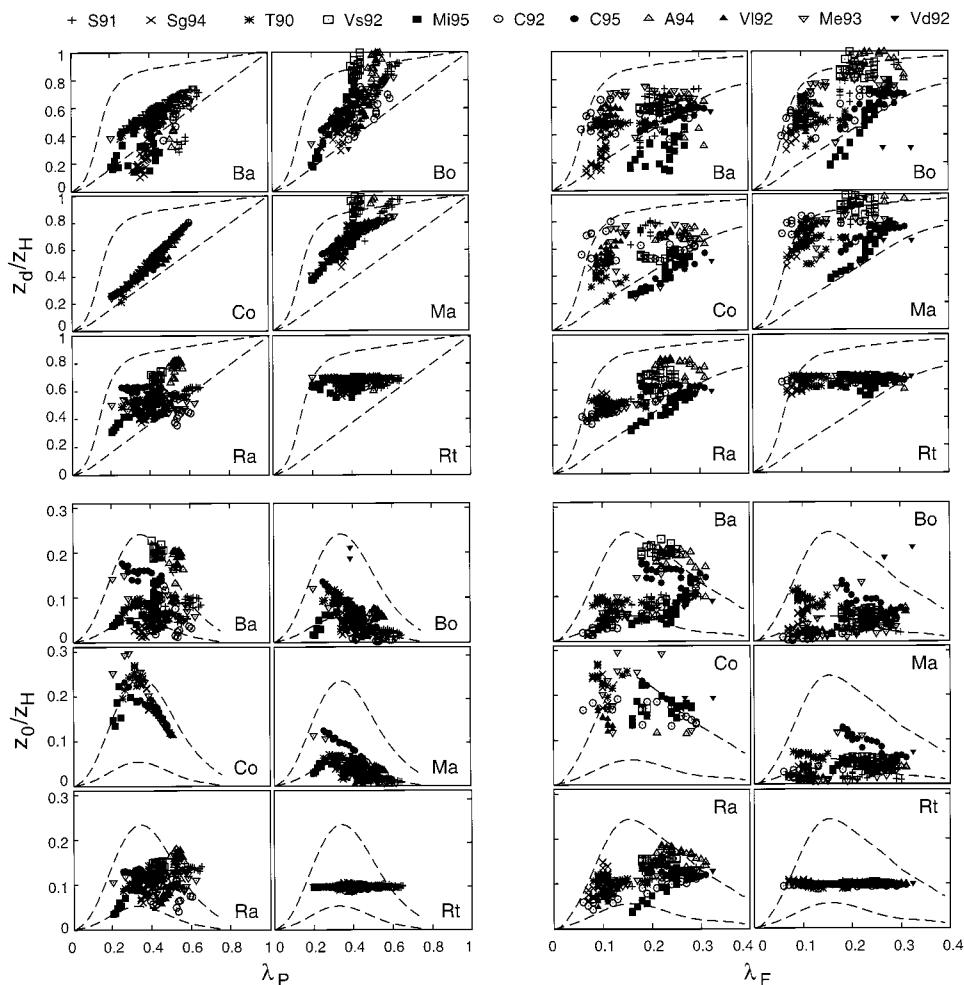


FIG. 5. Values of  $z_d/z_H$  and  $z_0/z_H$  for all 11 urban sites, calculated using the Bottema (Ba, Bo), Counihan (Co), Macdonald (Ma), Raupach (Ra), and rule-of-thumb (Rt) methods. (left) All methods plotted as a function of  $\lambda_P$ ; (right) surface described by  $\lambda_P$ . Top groups of six in each column are  $z_d/z_H$ , and lower groups of six are  $z_0/z_H$ . Envelopes contained by the curved dashed lines define the reasonable limits outlined in Fig. 1.

cept for C95, A94, and the high-rise downtown site Vd92.

The height-normalized values (Fig. 5) yield quite different outcomes using the different methods (again only Ba, Bo, Co, Ma, Ra, and Rt are shown). Visual assessment suggests that the Bo, Ba, and Ra methods perform best; all or a high proportion of their predictions lie within the reasonable zone. Further, they all demonstrate a central trend that declines at higher densities as expected. Here Co shows the desired peak, but the majority of its estimates lie above the reasonable zone. The Le and Ko approaches (not shown) give similar results; both perform well on the rising portion of the trend with density, but, rather than peak and decline, they continue to climb, and become increasingly unrealistic at high densities. In the range of North American morphometries represented in our database Rt with  $f_0 = 0.1$  would perform well, but obviously would fail at smaller and larger densities than these.

*c. Blending height ( $z_r$ )*

Predicted values of  $z_r$  (Fig. 4c) cover quite a wide range of absolute values, but values between 15 and 40 m are typical for residential sites. Larger values are predicted for central city sites. The blending height  $z_r$  gives some idea of the lowest height at which a surface layer may be expected to exist over such urbanized terrain. Since the dimensions of the upper extent of a surface layer depend on fetch requirements, which typically are 100–300 times the measurement height, it is obvious that a true surface layer may not always be present, especially over areas where land cover changes at scales less than several kilometers.

*d. Aerodynamic conductance ( $g_{aM}$ )*

Because they are so rough, cities exhibit large conductances. Therefore, they facilitate turbulent exchange

better than do most other types of smoother terrain. The predicted values for the residential and light industrial sites (Fig. 4d) at the height ( $3z_H - z_d$ ) mostly lie in the range  $20\text{--}100\text{ mm s}^{-1}$  with a median near  $65\text{ mm s}^{-1}$ . Values for the old central city site (Me93) also have a median near  $65\text{ mm s}^{-1}$ . The high-rise downtown (Vd92) values of about  $70\text{ mm s}^{-1}$  are unusually low; this result may be because only the Ba  $z_0$  was used and the reference height is very large ( $>80\text{ m}$ ). If we standardize the height scale by using  $(z_s - z_d)$  with sensor height  $z_s = 50\text{ m}$  for all sites, then these estimates translate into average  $C_D$  values of about  $0.8 \times 10^{-2}$  for the residential and warehouse sites and about  $1.6 \times 10^{-2}$  for the old central city site in Mexico City (Table 6). The Vancouver downtown site is hard to estimate, but may be between  $3 \times 10^{-2}$  and  $5 \times 10^{-2}$ .

## 6. Micrometeorologically determined aerodynamic characteristics of cities

Over the range of morphometric conditions found in North American cities the methods give significantly different values (Fig. 4). By themselves these results provide no objective basis for selecting one morphometric method over another; only general remarks can be made as to whether or not they look reasonable. As with any model validation, we appeal to the degree of agreement between prediction and direct observation: in this case, a comparison between modeled values and those obtained from analysis of wind measurements. Even then we cannot say which is correct because both morphometric and wind-based approaches to estimate/measure  $z_0$  and  $z_d$  in cities possess significant sources of error.

In general it is fair to say that, when working over other surfaces, most meteorologists consider that high-quality micrometeorological estimates represent the "standard." However, as Raupach et al. (1991) note, even over less heterogeneous terrain than cities, wind-based estimates (especially profile methods) are known to be inaccurate. Grimmond et al. (1998) also conclude that profile methods are suspect at a residential site in Chicago. This inaccuracy leaves turbulence-based approaches as the "best" source of field estimates.

A systematic review of field-based and model studies relevant to urban areas was conducted to assemble a database against which the morphometric results could be compared. Selection of high-quality data was governed by the following criteria, based on those of Wieringa (1993) and Bottema (1997).

- 1) *Terrain*. The site should be relatively flat.
- 2) *Tower construction*. Tower construction is slender and open enough to avoid wake effects near the instruments. Instrument booms are of sufficient length relative to the tower dimensions to ensure that there is no interference from the tower.
- 3) *Instruments*. Instruments possess appropriate response characteristics for mean wind or turbulence measurements.
- 4) *Measurement heights*. For real-atmosphere studies the lowest level must be greater than  $z_r = z_H + 1.5D$  and the highest level must be inside the internal boundary layer ( $\delta$ ) of the surface of concern. For wind tunnel studies Bottema (1997) uses the criteria  $z_{\min} > 2z_H$  and  $z_{\max} < 0.25\delta$ . Since it is necessary to have  $z_{\max}/z_{\min} > 2$ , it follows that the boundary layer depth requirement is  $\delta/z_H > 16$ . If profile methods are used, all instruments must be mounted in the constant flux layer of the relevant surface.
- 5) *Instrument spacing*. There are at least three instrument levels for profile studies, spaced at appropriate intervals.
- 6) *Sampling period*. Mean profiles and turbulent quantities are averaged over a sufficient time period.
- 7) *Stability*. Information on atmospheric stability is sufficient to establish that conditions were neutral or to allow stability corrections to be applied.
- 8) *Fetch*. Upstream distance of flow over surface of similar roughness is sufficient, and there are no anomalous structures nearby (a detailed map or photograph of the surroundings is most helpful). Bottema (1997) states a fetch requirement on the order of 1:250.
- 9) *Inclusion of  $z_d$* . Analysis to obtain roughness lengths must incorporate a zero-plane displacement.

Application of these criteria to an original total of more than 60 field studies with urban roughness estimates reduced the total to only 9. Those studies that pass the criteria are listed in Table 3, and Table 4 is the list of 14 accepted scale model (usually wind tunnel) studies. Field studies that were considered but rejected are listed in appendix B. These lists, while comprehensive, are not exhaustive.

The primary reasons (criteria) why studies were rejected are also given in appendix B. The most common problems were failure to include  $z_d$  in the analysis and the absence of sufficient information about the surface character of the site. As Bottema (1997) notes, strict implementation of more restrictive criteria results in rejection of virtually all available data. Our accepted field studies include less than half those in Wieringa's (1993) Table VII, but the overall number in our Table 3 is greater due to the addition of recent work. Only three of the accepted studies employ wind profiles with multiple anemometer levels. Data from some studies have been reanalyzed and are incorporated in the lists. Several studies might have been added if adequate site information had been provided (e.g., Greaves 1962).

The accepted data, nondimensionalized by the mean height of the elements, are plotted in Fig. 6 together with the reasonable curves and envelopes suggested in Fig. 1. To aid interpretation, the scale model and field results are presented separately. Each also is plotted versus the two main measures of roughness density.

The overall result conveyed by Fig. 6 is disappointing. Despite careful screening of data to retain only those of high quality, well-defined relations of the type discussed in section 1 are not evident. The scatter of  $z_d$  values from model studies is particularly marked, with about half the points lying outside the envelope. The  $z_d$  estimates from field studies are notable for their sparseness, the limited range of roughness densities they cover, and the large scatter, with half of the points outside the envelope. The  $z_0$  results conform better with expectation, especially the field set, but no clear peak is evident. Figure 6 also illustrates that the choice of surface descriptor, here  $\lambda_p$  or  $\lambda_F$ , makes a large difference [a conclusion also reached by Grimmond et al. (1998)]. It appears that  $\lambda_F$  is a more discriminating measure, drawing out a wider range of densities.

The features evident in Fig. 6 lead to four main conclusions. First, the "control" and simplicity thought to be provided by scale modeling is not evident. Therefore, this approach does not represent a panacea to enable study of urban roughness free of complications. Bottema (1997) and J. Finnigan (1997, personal communication) both note that the physical dimensions of even the largest wind tunnels often fail to provide sufficient fetch or boundary layer height to extract the logarithmic profile parameters without significant error. As a result, when considering measured wind profile parameters, we tend to favor the variable but authentically complex results of field studies, especially those using turbulence-based methods. Second, we tend to favor morphometric methods that incorporate  $\lambda_F$ , but we reiterate the need for a more comprehensive descriptor (appendix A). Third, while insensitive to surface form, the simple rule-of-thumb measures (especially  $Rt_0$ ) have some utility in the range of morphometry possessed by real cities. Fourth, the absence of clear trends between roughness density and either  $z_d$  or  $z_0$  in Fig. 6 suggests that even the best available observations do not provide a standard against which morphometric methods can be tested.

## 7. Comparison of measured and predicted values

Despite the fact that convergence between measured and modeled roughness estimates is no assurance of the validity of either approach, such comparison is virtually the only recourse we have to assess the reasonableness of results, beyond the heuristic arguments underlying the construction of Fig. 1. So, despite both the lack of expected trends and the sparse and scattered nature of the observed set, the field data (Table 3 and Fig. 6) were compared statistically with their corresponding morphometric estimates. The results are tabulated in Table 5 and are plotted in Fig. 7. Note that the number of observations that are available to conduct statistical analyses is often very small. The numbers of cases ( $n$  in Table 5) vary for the individual models because either the input data are not available (e.g., Bo) or the rough-

ness density of the surface is beyond the limits of applicability of the model (e.g., Ku).

Considering  $z_d/z_H$ , the observed mean value for the full set of field data ( $n = 31$ ) is 0.54; that is, if we hypothetically assume  $z_H = 10$  m then mean  $z_d = 5.4$  m. For the scale model set ( $n = 111$ ) the corresponding mean is 0.48. These values are smaller than the rule-of-thumb  $f_d$  value of 0.7 that we chose in section 1, but they straddle the 0.5 value suggested by Hanna and Chang (1992). In general, most of the models underpredict  $z_d$  when  $\lambda_p < 0.2$ ;  $Ra_d$  has the best performance at low  $\lambda_p$ . Using the  $r^2$ , rmse, and  $D$  statistics and the ratios of the predicted to observed mean that are defined and presented in Table 5, the overall rank order of the methods evaluated against the field data is probably  $Bo_d$ ,  $Ra_d$ ,  $Ma_d$ ,  $Ba_d$ ,  $Co_d$ , and  $Ku_d$ . That said, it is difficult to be enthusiastic about any one method, based on the statistics and the sparse plots of Fig. 7. Here  $Bo_d$  and  $Ra_d$  are best correlated with the observations. But  $Bo_d$  is based on only 15 values and  $Ra_d$  only explains 24% of the variance (however, the explanations provided by the rest are considerably poorer still). The  $Ra_d$  method possesses the smallest rmse, but even so, its magnitude means that for a hypothetical  $z_H = 10$  m the method is able to predict only that  $z_d$  is somewhere in the range between 3.5 and 6.7 m. In addition to having the highest  $r^2$  value,  $Bo_d$  has the highest Willmott  $D$  score and the second best rmse. When similar comparisons to these are made using the scale model data, all morphometric models perform as poorly or worse (Table 5).

The corresponding results for  $z_0/z_H$  also are weak (Table 5) and the relative difference between the modeled and measured values is an order of magnitude larger than for  $z_d/z_H$  (see Fig. 7). The observed mean for both the full field set ( $n = 54$ ) and the scale model data ( $n = 127$ ) is 0.08. Again this is in reasonable agreement with the rule-of-thumb  $f_0 = 0.1$  recommended by Hanna and Chang (1992). On the basis of the statistical measures given in Table 5, the probable ranking of the methods using the field set is  $Ra_0$ ,  $Ku_0$ ,  $Ba_0$ ,  $Ma_0$ ,  $Le_0$ ,  $Co_0$ ,  $Bo_0$ , and  $Ko_0$ . The  $Bo_0$  and  $Ra_0$  models perform the best when evaluated against the scale model data. Again the scatterplots visually confirm the lack of correlation (Fig. 7). Both  $Ku_0$  and  $Co_0$  show consistent bias toward values that are too high in comparison with the observed mean. The  $Ma_0$  method tends to be too small at larger values of  $\lambda_p$  ( $>0.4$ ). In all cases the rmse for model evaluations is poorer compared against the scale model than against field data.

These results provide little basis for recommendations concerning which morphometric methods should be used. This failure is not surprising given the unsuitability of the observed data, as noted in section 6. Therefore, in addition to these statistics, our recommendations include considerations such as

- ease of implementation (input requirements),



TABLE 3. (Continued)

City (site), surface description	Method <sup>a</sup> (no. of cases, season)	$z_0$ (m)	$z_d$ (m)	$z_H$ (m)	$z_d/z_H$	$\lambda_p$	$\lambda_r$	$\lambda_s$	UTZ <sup>b</sup>	Source
Worcester, MA, mixed density—houses and university	Es (13)	2.13 ± 0.26	Na	14.4	2.1	0.38	0.13	0.6	Do6	Yersel and Goble (1986)
Zurich, Switzerland (Anwand), high densi- ty—< 5-story row apartments, shops	Tv, Es (5)	Na	9.0–16.5	16.8–18.0	1.3–1.6	0.22–0.39	0.25–0.61	1.0	A1/A2	Rotach (1994) <sup>c</sup>

<sup>a</sup> Lw, log wind profile analysis; Su, standard deviation of wind speed; Es, turbulent stress from eddy correlation; Tv,  $z_d$  from temperature variance [see Grimmond et al. (1998) for details of all methods]. Season: F, fall; S, summer; W, winter.  
<sup>b</sup> UTZ, urban terrain zones according to Ellefsen (1990–91) classification.  
<sup>c</sup> The  $z_0$  estimated from  $u_c$  and surface geometry information given in the paper.  
<sup>d</sup> Data reported for 43.1-m measurement height; for additional data see Grimmond et al. (1998).  
<sup>e</sup> The  $\lambda_r$  from Bottema (1995b);  $z_0$  for the fall appears to have been reported in error; value obtained from figures given in the report.  
<sup>f</sup> Modified by Bottema (1995b).  
<sup>g</sup> Additional data provided by the author. Only sectors 46°–270° are used.

- applicability across the full range of typical urban morphometries,
- choice of descriptor of surface form (roughness density), and
- conformity with the suggested curves and envelopes of reasonableness drawn in Fig. 1.

Taking these characteristics into account, we suggest the following rank ordering of morphometric methods that can be used to predict both  $z_d$  and  $z_0$ .

- Bo, designed for regular building arrangements with  $\lambda_p > 5\%$ . The statistics for both zero-plane and roughness length place the method in the upper half of the individual rankings and none of the individual statistics gives unacceptable values. The method is not limited with respect to range of surface form, it explicitly incorporates the possibility of different spatial arrays, and, when applied to the cities in our North American database, it generates estimates that mostly conform with the reasonable limits of Fig. 1. Its greatest drawback is its demanding set of input requirements as compared to those of any other method. Until the widespread availability of sufficiently detailed urban GIS is realized, this feature is likely to restrict this method to experimental studies.
- Ra, designed for random building arrangements and sparse random canopies. Again, the majority of statistics for both  $z_0$  and  $z_d$  are acceptable, although the  $D$  statistic for roughness length is low. Input requirements are relatively simple, the method applies across the full range of densities, the surface is described using  $\lambda_r$ , and the estimates generated for North American cities mainly fall within the limits proposed here (Fig. 5). The Ra model requires four parameters to be specified, three of which influence only  $z_0$ . Tests of the Ra model that vary these parameters and use Bottema's (1997) method as an alternative way to determine the wake length parameter result in no notable improvement in model performance.
- Ma, a modification of Le derived from fundamental principles for obstacle arrays. The statistics place this method in the middle of the rankings. It has the advantage that it is applicable across the full range of densities and that the estimates generated for the North American cities are mostly reasonable. As the authors state, the model coefficients  $\alpha$  and  $\beta$  can be calibrated, but this calibration was not attempted here. The most appropriate parameters were taken a priori from the original study, in an attempt to use the method in a more objective form.
- Ba, a simplified version of Bo designed for irregular building arrangements. Again, while the absolute values of the statistics are disappointing, this method scores almost as well as the previous three, with the exception of the low  $D$  value for  $z_d$ . The estimates generated from the North American cities (Fig. 5) are generally low for  $z_d$  but are among the best for  $z_0$ . The input requirements are reasonably simple (com-

TABLE 4. Wind tunnel and other scale model studies used to evaluate morphometric methods. For experimental details refer to the source indicated.

Original author	Source of data used
Cook (1976)	Bottema (1995b, 1997)
Counihan (1971)	Bottema (1995b, 1997)
Iqbal et al. (1977)	Bottema (1995b, 1997)
Hussain and Lee (1980)	Bottema (1995b, 1997), Hussain and Lee (1980)
Kutzbach (1961)	Fang and Sill (1992), Kutzbach (1961)
Liedtke (1992)	Bottema (1995b, 1997)
Mulhearn (1978)	Bottema (1995b, 1997)
O'Loughlin and MacDonald (1964)	Bottema (1995b, 1997), Fang and Sill (1992)
Raupach et al. (1980)	Bottema (1995b, 1997), Fang and Sill (1992)
Schlichting (1937, 1968)	Bottema (1995b, 1997), Fang and Sill (1992)
Styles (1997)	Styles (1997)
Theurer (1993)	Theurer (1993)
Tieleman et al. (1978)	Bottema (1995b, 1997), Fang and Sill (1992)
Visser (1987)	Bottema (1995b, 1997)

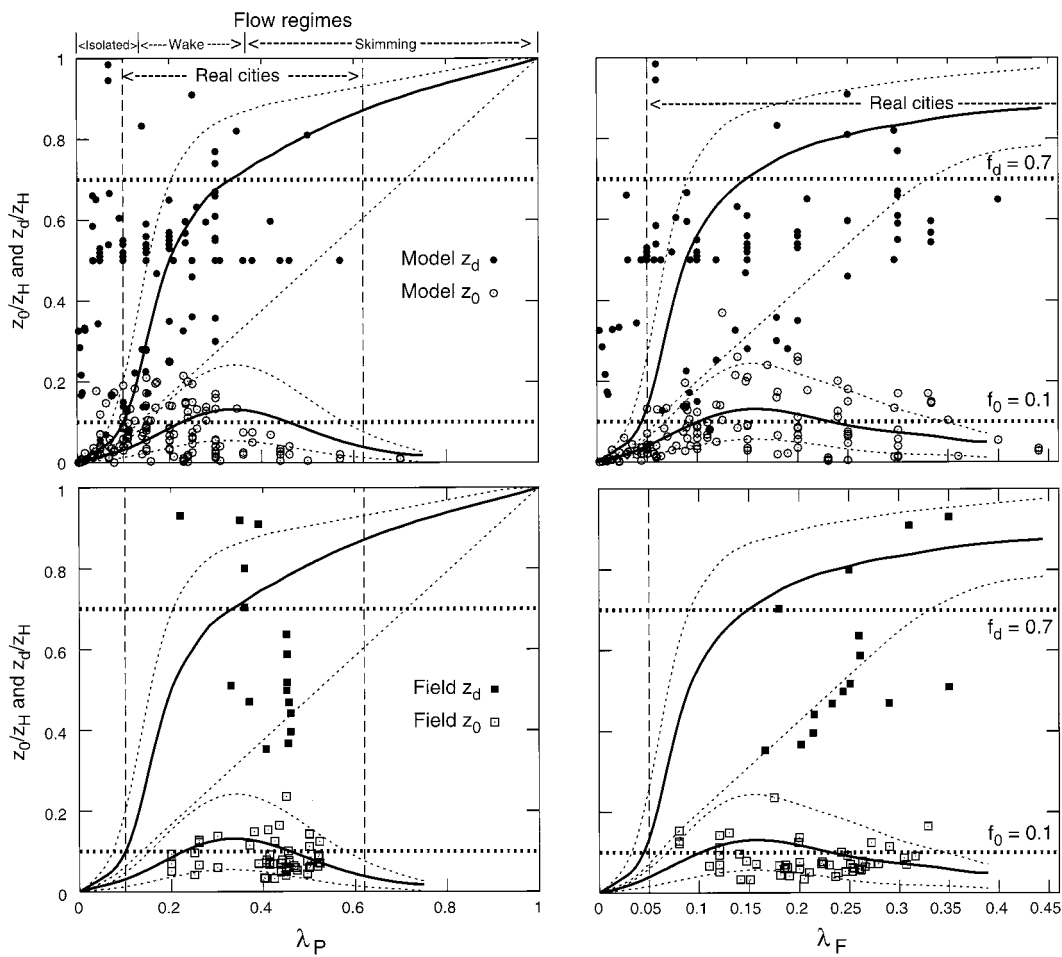


FIG. 6. All available data from scale model (mostly wind tunnel) and field (full scale) studies of  $z_d$  and  $z_0$  that fulfill the criteria outlined in section 6 and listed in Tables 3 and 4. Panels are organized with scale model results in the top two panels and field results in the bottom two. The left two panels use  $\lambda_P$  to describe the surface form, and the two at the right use  $\lambda_F$ . Envelopes contained by the curved dashed lines define reasonable limits. The vertical dashed lines show the range of real-city roughness densities.

TABLE 5. Linear correlation statistics showing degree of agreement between morphometric and field-derived or scale model values of  $z_d/z_H$  or  $z_0/z_H$ ;  $n$ , sample size;  $O$ ,  $P$ , observed and predicted means of the dataset, respectively;  $r^2$ , coefficient of determination;  $a$ ,  $b$ , slope and intercept of linear regression, respectively; rmse, root mean square error;  $R_{SY}$ , systematic error;  $R_{USY}$ , unsystematic error;  $D$ , Willmott index of agreement (Willmott 1981). All values are dimensionless.

Method	Field data										Scale model data									
	$n$	$O$	$P$	$r^2$	$b$	$a$	rmse	$R_{SY}$	$D$	$n$	$O$	$P$	$r^2$	$b$	$a$	rmse	$R_{SY}$	$R_{USY}$	$D$	
$z_d$	Ba <sub>d</sub>	31	0.54	0.53	0.01	0.03	0.52	0.19	0.17	0.09	0.38	0.48	0.37	0.10	0.23	0.23	0.17	0.15	0.55	
	Bo <sub>d</sub>	15	0.46	0.62	0.38	0.43	0.42	0.18	0.17	0.07	0.55	0.49	0.29	0.10	0.13	0.30	0.24	0.19	0.52	
	Co <sub>d</sub>	31	0.54	0.47	0.01	0.05	0.44	0.23	0.19	0.13	0.45	0.48	0.25	0.08	0.10	0.32	0.26	0.19	0.49	
	Ku <sub>d</sub>	11	0.48	0.66	0.09	-0.04	0.69	0.28	0.28	0.03	0.41	0.47	0.56	0.10	0.45	0.21	0.17	0.12	0.55	
	Ma <sub>d</sub>	31	0.54	0.61	0.01	0.04	0.59	0.22	0.19	0.11	0.41	0.48	0.39	0.10	0.21	0.25	0.15	0.20	0.56	
	Ra <sub>d</sub>	31	0.54	0.52	0.24	0.19	0.41	0.16	0.15	0.06	0.55	0.50	0.43	0.18	0.29	0.19	0.15	0.11	0.60	
$z_0$	Ba <sub>0</sub>	54	0.08	0.06	0.03	-0.09	0.07	0.05	0.05	0.02	0.33	0.08	0.39	0.42	8.73	0.98	0.64	0.75	0.16	
	Bo <sub>0</sub>	44	0.08	0.07	0.00	-0.04	0.07	0.06	0.04	0.04	0.36	0.06	0.08	0.09	0.26	0.06	0.05	0.04	0.56	
	Co <sub>0</sub>	47	0.08	0.18	0.01	0.13	0.17	0.12	0.11	0.06	0.32	0.08	0.76	0.33	14.94	1.91	1.20	1.49	0.08	
	Ko <sub>0</sub>	54	0.08	0.10	0.00	-0.02	0.11	0.05	0.04	0.02	0.38	0.08	0.16	0.31	2.73	-0.06	0.32	0.15	0.29	
	Ku <sub>0</sub>	10	0.09	0.21	0.12	0.37	0.18	0.13	0.12	0.03	0.34	0.09	0.52	0.33	9.22	1.20	0.74	0.95	0.12	
	Le <sub>0</sub>	54	0.08	0.10	0.02	-0.13	0.11	0.06	0.05	0.03	0.29	0.08	0.08	0.03	0.18	0.07	0.10	0.06	0.08	
	Ma <sub>0</sub>	54	0.08	0.04	0.01	-0.05	0.05	0.06	0.06	0.02	0.39	0.08	0.59	0.32	13.63	1.72	1.03	1.39	0.09	
	Ra <sub>0</sub>	54	0.08	0.11	0.07	-0.13	0.12	0.06	0.05	0.02	0.30	0.08	0.08	0.10	0.16	0.07	0.06	0.04	0.52	

pared with Bo) and the method can be applied across the full range of real-world morphometries.

- Co, a parameterization of experimental data. In most respects this method scores well for  $z_d$  but it overpredicts the magnitude of  $z_0$ . It is restricted in terms of applicability.
- Ku, a parameterization of experimental data. This approach is limited severely by its restriction to a relatively small range of roughness densities. As a result, it cannot be recommended for general use in urban areas. In addition,  $z_0$  estimates from Ku are consistently too large.

The two methods that predict  $z_0$  but not  $z_d$  (Ko, Le) give some of the best  $z_0$  results (Table 5). Nevertheless, they cannot be recommended for general use due to their failure to predict declining roughness at large densities (Fig. 3). This failure limits their use to urban forms that generate nonskimming flow. Further, since neither method provides an equation for  $z_d$ , it is necessary to use one of the other methods, which could compound errors. Despite these negative features, if the urban morphometry lies within the correct range (i.e.,  $\lambda_F < 0.25$ ) the  $z_0$  estimates probably are acceptable. This finding is relevant because, to date, Le is probably the most widely used morphometric method in urban studies. The extension of Le to produce Ma is a significant improvement.

The very simple Rt formula works quite well in the mean for both  $z_d$  and  $z_0$ . However, because its formulation includes no recognition of density it cannot respond to the effects of packing. This deficiency becomes increasingly problematic for  $z_d$  because of the anticipated slope of the  $f_d$  curve with density (Fig. 1). It is less of a problem for  $z_0$  because of the behavior of the  $f_0$  curve with density; but  $Rt_0$  increasingly overestimates roughness at very high and very low densities and fails to pick up the roughness peak. Our survey of scale model and field results supports Hanna and Chang's (1992) recommendation that  $f_d \sim 0.5$  and  $f_0 \sim 0.1$  in urban areas. However, since our survey is biased toward lower densities, a better recommendation for  $f_d$  may be 0.5 for low-, 0.6 for medium-, and 0.7 for high-density urban sites.

### 8. Recommended values

In summary, there are remarkably few high-quality measurements of urban roughness parameters (section 6). Moreover, it is not clear that this situation is likely to change in the foreseeable future because, even with the best available instrumentation, the natural heterogeneity of urban sites and the sensitivity of analyses to small errors often lead to an unreliable outcome (Grimmond et al. 1998; Schaudt 1998). This lack of a sizable and authoritative body of measured values means that there is no credible standard against which to validate morphometric formulas.

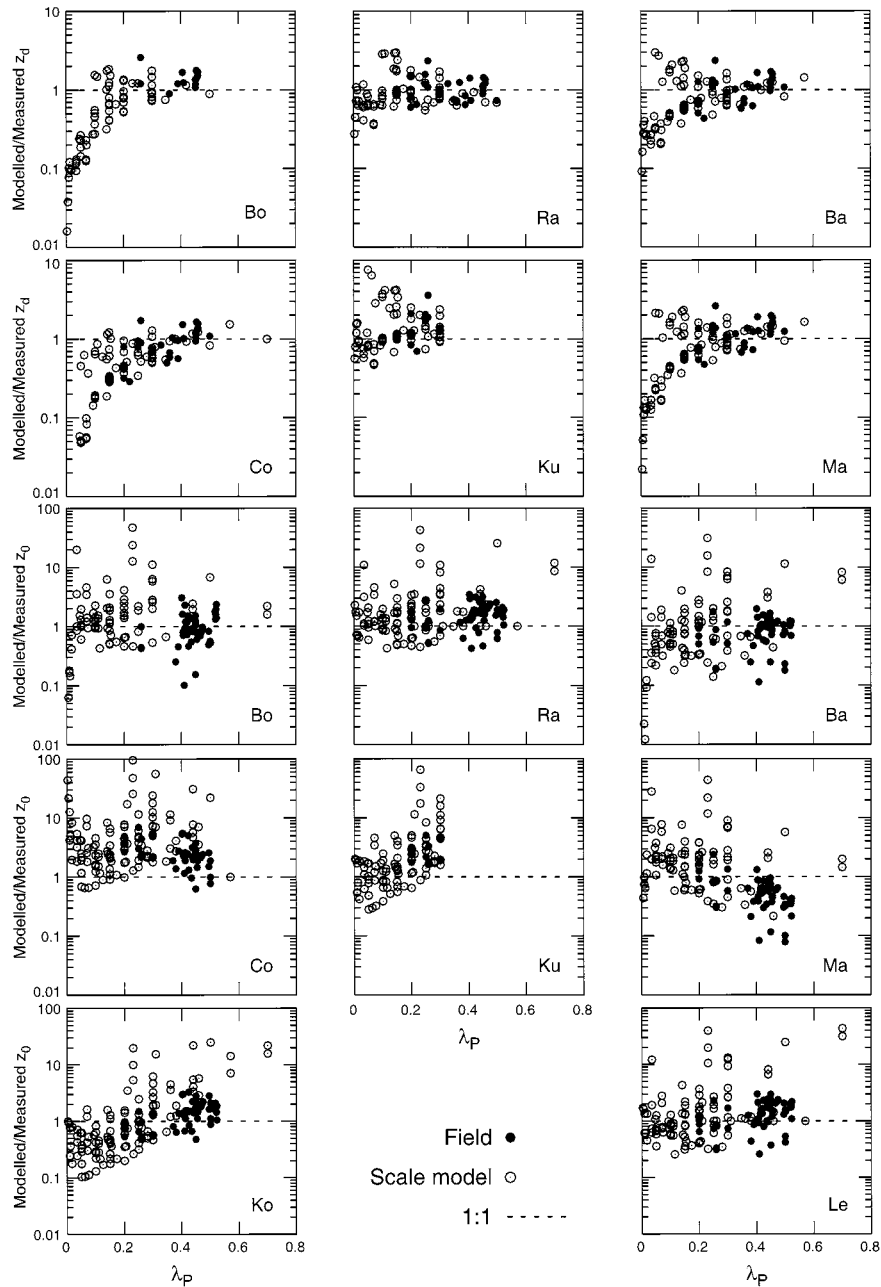


FIG. 7. The ratio of measured (scale model and field) to modeled values of  $z_d/z_H$  (first two rows) and  $z_0/z_H$  (remaining rows) according to the morphometric method used. Perfect agreement between measured and modeled data is unity (horizontal dashed lines). Note the logarithmic scale of the y axis.

Given this unsatisfactory state of affairs, one might ask to where modelers, those calculating urban air pollution dispersion, or others can turn to obtain values of urban aerodynamic characteristics. In the unlikely event that measurement is contemplated, turbulence-based approaches are favored over those involving multilevel profiles of anemometers [see further discussion in Grimmond et al (1998)]. If morphometric analysis is envisaged, our recommendations about choice of method are

given in section 7. Given the errors involved in *both* measurement and morphometric analysis and the lack of an overall standard, it is not clear which class of method is favored on grounds of accuracy. That being so, the facts that morphometric methods are relatively simple, are cost-effective, and yield values for all directions around a site (section 1) are attractive.

If neither measurements nor morphometric analysis can be conducted, first-order estimates can be obtained

TABLE 6. Typical roughness and other aerodynamic properties of homogeneous zones in urban areas, ordered by height and density.

Urban surface form	$\overline{z_H}$ (m)	$\overline{z_d^a}$ (m)	$\overline{z_0^a}$ (m)	$\overline{g_{aM}^b}$ (mm s <sup>-1</sup> )	$\overline{C_D^b}$ ( $\times 10^{-2}$ )
Low height and density					
Residential—one- or two-story single houses, gardens, small trees. Mixed houses and small shops. Warehouse, light industrial, few trees.	5–8	2–4	0.3–0.8	30–50	0.6–1.0
Medium height and density					
Residential—two- and three-story large or closely spaced, semidetached and row houses, large trees. Less than five-story blocks of flats with open surroundings. Mixed—houses with shops, light industry, churches, schools.	7–14	3.5–8.0	0.7–1.5	45–75	0.9–1.5
Tall and high density					
Residential—closely spaced < six-story row and block buildings or major facilities (factory, university, etc.), town center.	11–20	7–15	0.8–1.5	50–80	1.0–1.6
High-rise <sup>c</sup>					
Urban core or suburban nodes with multistory tower blocks in dense urban surroundings. Major institutional complexes.	>20	>12	>2.0	>90	>1.9

<sup>a</sup> Sites with above- (below-) average tree cover will have larger (smaller)  $\overline{z_d}$  and  $\overline{z_0}$ . Sites with deciduous tree cover will have 20%–30% smaller  $\overline{z_0}$  values during the leaf-off period. Smaller values are likely if the fetch direction is along a major road. Values greater than or less than these can arise because of the absolute height of the roughness elements.

<sup>b</sup> Assumes neutral stability,  $z_s = 50$  m and  $u = 5$  m s<sup>-1</sup>.

<sup>c</sup> There are almost no measured values in this class; therefore, values have little support.

from tables of typical values. Table 6 here extends Table VIII of Wieringa (1993) by recognizing four types of urban roughness terrain defined on the basis of the height and packing density of the roughness elements. Each of the accepted sites from our survey is described in terms of such densities (see the first column in Table 3). The high-rise category applies to those portions of modern cities that have clusters of tall towers of offices or apartments often irregularly distributed, that jut up above one of the other three types. Table 6 associates each of these urban surface types with a typical range of mean roughness heights and the corresponding range of values for the roughness-related parameters:  $\overline{z_d}$ ,  $\overline{z_0}$ ,  $\overline{g_{aM}}$ , and  $\overline{C_D}$ . To establish comparability,  $\overline{g_{aM}}$  and  $\overline{C_D}$  assume a standard height of measurement ( $z_s = 50$  m) and wind speed ( $u_{ref} = 5$  m s<sup>-1</sup>). The choice of  $\overline{C_D}$  values also benefited from the survey of measured  $u_*^*/u$  ( $=C_D^{1/2}$ ) values for cities that was prepared by Roth (1999). Values in the high-rise class are without support from field data, because there are none. They are largely based on morphometric estimates, theory, and intuition, and should therefore only be used as first-order indications. It may even be argued that flow around such irregular arrays cannot conform with the requirements of equilibrium flow and the logarithmic law.

Comparing these urban  $\overline{z_0}$  values with those of natural surfaces given by other tables of typical roughness (e.g., Oke 1987; Stull 1988; Raupach et al. 1991; Garratt 1992; Wieringa 1993) confirms that cities and forests are near the top end of the scale. For example, broadly typical values of  $\overline{z_0}$  (m) are for water, 0.0002; short

grass, 0.01; crops, 0.1; and forests, 1–2. Using the same  $\overline{z_s}$  and  $u_{ref}$  as specified in Table 6, these roughness lengths translate into the following  $\overline{g_{aM}}$  values (mm s<sup>-1</sup>): water, 5; short grass, 11; crops, 21; and forests, 62–96 (e.g., Szeicz 1974; Stewart 1984). Therefore, ceteris paribus, the drag exerted and the efficiency of above-roof diffusion and transport are greater over cities than for most rural surfaces except forests, and downtown cores of modern cities probably exceed forest values. Nevertheless, it should not be overlooked that  $\overline{z_0}$  for the first urban category in Table 6, which occupies the greatest area of most North American cities, is not as large as that for a mature forest, and that only the fourth category of urban roughness can be called unusually rough. Notice also that within a single city it is possible to find almost a fourfold range of  $\overline{z_0}$ ,  $\overline{g_{aM}}$ , and  $\overline{C_D}$  if the full range of morphometry classes are represented.

For the medium and tall classes in Table 6  $\overline{z_0}$  varies relatively little. This lack of variation is because, although skimming flow generates less roughness, this effect is partially compensated for by the greater absolute height of the elements. The tall and medium classes are thus mainly differentiated by  $\overline{z_d}$ . We think this fact is important enough to warrant recognition, but if  $\overline{z_0}$  alone is required then these two classes can be merged. It has been mentioned (J. Wieringa 1998, personal communication) that the urban roughness survey we present here is not neatly congruent with the roughest classes of the well-established Davenport roughness classification (Davenport 1960; Wieringa 1992). This lack of agreement is the subject of ongoing discussion.

We also forward a simple scheme to aid users to obtain first-order estimates of urban roughness parameters by using Table 7 and Fig. 8 together. This approach avoids measuring multiple absolute dimensions and instead uses qualitative (essentially visual) assessment of urban form along with nondimensional roughness coefficients ( $f_d$  and  $f_0$ ). The first three categories in the first column of Table 7 broadly correspond to those combinations of roughness density that generate the isolated, wake interference, and skimming flow regimes, respectively, and the fourth category is urban morphometry that results in what might be called "chaotic flow." While these densities can be quantified by use of aspect ratios such as  $\lambda_p$  or  $\lambda_s$  (see Fig. 2), it probably is much easier to classify urban morphometry from aerial photography. In particular, oblique-angle photographs quickly enable an observer to assess the mix of elements, their packing, and both their relative and absolute height (e.g., number of stories). Conceptually this approach mirrors that successfully employed in wind-loading studies (e.g., Newberry and Eaton 1974), and advocated by the Environmental Protection Agency in air quality models (see discussion in Petersen 1997).

Ellefsen (1990–91) has devised a scheme that uses aerial photography to classify the physical structure of cities into what he calls urban terrain zones (UTZ). The method has several positive attributes for use in urban climate studies; namely, it is based on physical structure, not function such as land use; it requires only visual assessment, not complex dimensions; and it is applicable to cities all over the world (Cionco and Ellefsen 1998). Ellefsen's scheme identifies 17 types of UTZ; each can be classified via a template that consists of a written description, a photograph, and both plan and side-elevation drawings. We adapt the scheme for our purpose by assigning each UTZ to one of the four roughness categories in Table 7 and consolidating them as a matrix of typical photographs in Fig. 8. To implement the scheme, a user (a) chooses an appropriate analog for their site from the photo matrix, (b) confirms that the plan and canyon geometries ( $\lambda_p$  and  $\lambda_s$ ) are appropriate, (c) estimates the mean element height  $\bar{z}_H$  (typically each story of a building represents about 2.5–3 m), and (d) calculates  $z_d$  and  $z_0$  from the  $f$  coefficients in the last two columns of Table 7. The  $f$  values in the chaotic flow row are little more than guesses based on morphometric expectations, because there are no acceptable field data. Another important caveat is that the scheme does not account explicitly for atypical amounts of vegetation at a site. As we have shown, trees can be a significant component of urban roughness.

## 9. Concluding remarks

This paper has concentrated on the nature, sensitivity, and size of aerodynamic parameters obtained using morphometric methods, especially in the context of the physical structure of parts of North American cities. It

uses sensitivity analysis to show that almost all morphometric formulas for  $z_d$  generate reasonable values (based on heuristic arguments). Similarly, most morphometric formulas for  $z_0$  predict intuitively reasonable values for small to medium roughness densities, but the methods of Lettau and of Kondo and Yamazawa fail at medium to large densities.

Detailed GIS surveys of 11 sites in 7 North American cities have been used to calculate several physical characteristics that are of interest to urban climate, including roughness element height, plan area density, frontal area index, canyon aspect ratio, and complete surface area. The GIS together with morphometric formulas are used to predict  $z_d$ ,  $z_0$ ,  $z_r$ , and  $g_{AM}$  for these sites. Only the methods of Bottema (both Bo and Ba), Raupach, and Macdonald et al. provide schemes that cover both  $z_d$  and  $z_0$  across the full range of surface morphometry found in such cities. The morphometric estimates show the potential to generate roughness characteristics for urban terrain, including its spatial variation, relatively easily.

In an effort to convert this potential into valid estimates, we sought confirmation using observed roughness characteristics. We conducted a comprehensive review of field and scale model studies in which roughness parameters were observed. Unfortunately, after application of quality control criteria, we find that very few studies are acceptable. As a result we judge there to be few credible estimates of urban  $z_0$  and almost none of  $z_d$ . Further, the results from those studies that are accepted do not show well-defined trends with roughness density. While including results from scale model studies significantly increases the number of available data points, it does not reduce the scatter or lead to a well-defined relation between measured roughness and indices of density (Fig. 6). It also suggests that there is a significant quality difference between data from field projects and data from scale models.

Describing the physical form of an inhomogeneous system such as a city is a nontrivial task. During this study we calculated several descriptors of surface form and density ( $\lambda_p$ ,  $\lambda_F$ ,  $\lambda_s$ , and  $\lambda_C$ ) and attempted to devise others of our own construction. Our conclusions are that (a) the choice of surface descriptor makes a real difference to the degree of success of relations between density and roughness characteristics; (b) none of the descriptors we used were able to capture fully the geometry appropriate for aerodynamic purposes; and (c) some of the problems with the morphometric models are attributable to these concerns.

There is poor statistical agreement between even the highest-quality measurements and the morphometric estimates of roughness parameters for cities. Part of this discrepancy is due to irreducible errors in observation and analysis of winds over inhomogeneous surfaces and in the necessary process of simplification of their geometric description. These uncertainties in both measurement and prediction mean that there is no standard

TABLE 7. Typical nondimensional roughness properties of homogeneous zones in urban areas, ordered by urban density and flow regime.

Urban surface density— Flow regime	UTZ (urban terrain zones <sup>a</sup> )	$\overline{\lambda_p}$ <sup>b</sup>	$\overline{\lambda_s} = \overline{z_H/W}$	$f_d = \overline{z_d/z_H}$	$f_0 = \overline{z_0/z_H}$
Low density—isolated flow Buildings and trees are small and widely spaced, e.g., modern single-family housing with large lots and wide roads; light industrial area or shopping mall with large paved or open space.	Do1, Do3–Do5	0.05–0.40	0.08–0.30	0.35–0.50	0.06–0.10
Medium density—wake interference flow Two- to four-story buildings and mature trees, elements of various heights occupy more than 30% surface area and create semiencloded spaces (street canyons, courtyards), e.g., closely spaced, large, and semidetached houses, blocks of apartments in open surroundings. Mixed houses with shops, light industry, churches, and schools.	A5, Dc3, Dc5, Do2	0.3–0.5	0.3–1.0	0.55–0.7	0.08–0.16 <sup>c</sup>
High density—skimming flow Buildings and trees closely packed and of similar height, narrow street canyons, e.g., old town centers, dense row, and semidetached housing, dense factory sites.	A1–A4, Dc2, Dc4	0.5–0.8	0.65–2.00	0.60–0.85	0.07–0.12
High-rise—chaotic or mixed flow <sup>d</sup> Scattered or clustered tall towers of different heights jutting up from dense urban surroundings, e.g., modern city core, tall apartment, major institution.	Dc1, Dc8, Do6	>0.4	>1	0.50–0.70	0.10–0.20

<sup>a</sup> UTZ codes are from Ellefsen (1990–91).

<sup>b</sup> Plan areas of buildings only.

<sup>c</sup> Largest values likely to apply to midrange of  $\lambda_p$  and  $\lambda_s$ .

<sup>d</sup> Unique distribution of major elements makes it difficult to generalize, except to expect that roughness is enhanced by addition of tall elements.

against which either set can be compared. Given this unsatisfactory circumstance, we opt to amalgamate both sets and use them to do the following.

- 1) To suggest that, of the morphometric methods, Bo, Ra, and Ba are probably the best that are currently available. Input requirements for the Bo method are likely to limit its use. The Ma model is an attractive alternative given its good performance and more readily available data requirements. Several other methods are useful but only apply to a limited range of roughness densities.
- 2) To develop tables of roughness parameters that are deemed to be representative of four different types of urban morphometry, which in turn are linked to the creation of four distinct flow regimes. Further, we suggest that these urban roughness types can be identified from the morphometric information contained in oblique-angle aerial photographs, leading to a simple visual means of obtaining first-order roughness estimates.

It seems natural, given the lack of high-quality data, to argue for more field and, perhaps, scale model studies. Unexpectedly, the performance of the models was generally poorer with respect to scale model data than to field data. However, given the inherent uncertainties and errors associated with current methods, it remains moot

whether such effort can improve greatly the state of affairs summarized here. This sobering fact does not mean that we cannot improve present practice, especially with respect to choice of roughness parameters incorporated in studies of urban diffusion and in mesoscale models of airflow and urban climate. First, all such work must account explicitly for existence of the urban canopy layer by incorporating a zero-plane displacement. Second, having accounted for  $z_d$ , the magnitude of the roughness length should be compatible with those in Tables 3 and 6. The morphometric approaches recommended in section 7 are appropriate, or, if necessary,  $z_0$  may be estimated with the visual scheme that combines Table 7 and Fig. 8 (or with Ellefsen's template). While these recommendations are elementary, a review of the urban modeling literature shows it to be replete with examples where  $z_d$  is omitted and input values of  $z_0$  are patently unreasonable (usually too large).

*Acknowledgments.* The assistance of the many people who aided with fieldwork, development of the surface databases, and provision of data is greatly appreciated. In particular, we would like to thank Dr. Catherine Souch for her contributions to many dimensions of this study; Dr. Richard Ellefsen and Dr. Alfred Siemens for providing several of the photographs forming Fig. 8; Dr. Marcel Bottema for discussion regarding the imple-

## Low



## Medium



## High



## High-rise



FIG. 8. Photographs of the physical nature of urban morphometry representing examples of the four urban roughness categories in Table 7. Urban terrain zone (UTZ) classes: (a) Do3, (b) Do3, (c) Do4, (d) Dc3, (e) Do2, (f) A5, (g) A2, (h) A1, (i) Dc2, (j) Dc1, (k) Dc1, and (l) Dc8. [Photo credits: (a) courtesy of Mining Company of Québec (Cartier); (b) TRO; (c), (d), (e), (h), (j) © R. Ellefsen; (f), (k) ©A. H. Siemens; (g) courtesy of H. Wanner; (i) courtesy of H. Saaroni; (l) courtesy of R. G. Kliass.]

mentation of his method; Dr. James Voogt for providing the surface database for the downtown site in Vancouver; Dr. Hans-Peter Schmid for assistance with FSAM; and Drs. John Finnigan, Robert Macdonald, Matthias Roth, Roland Stull, and Jon Wieringa for helpful discussion. We are grateful to the organizations and individuals who made observation sites and facilities available to us in the seven cities, especially Dade County Fairground (Miami), School of Mines (Mexico City), British Columbia Hydro and Power Corporation and Summer Equipment Ltd. (Vancouver), Drs. A. and G. McPherson (Tucson), Carmichael School District (Sacramento), Illinois Department of Transportation and State Police (Chicago), and California State Arboretum and San Gabriel Water District (Los Angeles). Funding was provided to SG by Southern California Edison, USDA Forest Service Cooperative Research Grants 23-526 and 23-546, and by Indiana University for a Faculty Research Grant and Faculty Fellowship; and to TRO by the Natural Sciences and Engineering Research Council of Canada.

## APPENDIX A

### North American Urban Morphology

#### a. Geometric characteristics

The surveys in the seven cities allowed calculation of several morphologic characteristics of significance in aerodynamic and other urban climate studies that are of value in themselves (Fig. A1). Such statistics have not readily been available previously. It is convenient to discuss the eight suburban residential sites (T90, Sg94, S91, Vs92, C92w, Mi95, C95, A94) as a group, separate from the light industrial (VI92) and downtown (Me93, Vd92) sites. Since no morphometric descriptor captures all dimensions of surface roughness, several are used in the literature (see Fig. 2 for definitions).

#### b. Height of roughness elements ( $\overline{z_H}$ )

The height of the roughness elements is the simplest first-order control on surface aerodynamic properties. Average height can be calculated in a number of ways—for example, as a straight geometric average or as a weighted average based on each roughness element's contribution to plan area ( $\lambda_p$ ) or frontal area index ( $\lambda_F$ ). Depending on the mix of buildings and trees, their relative heights, and their variation, the “average” height will differ. The heights given in Table 2 illustrate this fact. It shows the mean geometric heights for the buildings and trees separately and the  $\lambda_p$ - and  $\lambda_F$ -weighted averages for each of the study sites. Clearly, the numbers are different (varying by over a factor of 2 in the case of A94). Unless otherwise stated in subsequent discussion, it can be assumed that mean heights are  $\lambda_F$ -based values because that is the most appropriate measure for aerodynamic applications. The mean height (based on

$\lambda_F$ ) also is used to rank order the study sites in Table 2 and Figs. 4 and A1.

The group of eight single-family residential sites from six North American cities from very different climatic zones shows several interesting facts. First, the heights of their urban canopy layers are remarkably similar. Second, in absolute terms, that height is relatively low; mean building  $\overline{z_{bb}}$  values lie between 4.7 and 8.0 m, with a mean of 5.7 m. Third, at all but one of the residential sites (T90), the trees and shrubs on average are taller than the buildings; hence when trees are included, the final all-element urban  $\overline{z_H}$  estimate increases. The Mi95 estimate in Table 2 probably understates the role of trees compared with what is normal for this site. Hurricane Andrew in August 1992 damaged or destroyed many trees at this site; when they recover, the average height of the vegetation will be greater. Fourth, the variability of element height between sectors is relatively small; the standard deviation is less than 20% of the mean.

The mean height at the warehouse site VI92 is similar to that of residential sites but its standard deviation for the different sectors is even smaller. The central city sites, Me93 and Vd92, stand apart from all others. At Me93,  $\overline{z_H}$  is more than twice as high as at any other site except Vd92, which is almost twice as tall again. Height variability is also greater (about 30% at Me93).

#### c. Spacing of roughness elements ( $D$ )

When both buildings and trees are included, the mean spacing  $D$  between roughness element centroids ranges from  $\sim 20$  to 40 m at residential sites, with most close to  $\sim 25$  m (Fig. A1e). When individual sectors are looked at, the range across all sites is  $\sim 13$ –80 m, but only C92w has values greater than 55 m. Element spacing in the VI92 warehouse district is quite similar to that at residential sites, but in the central city the larger elements and sparse vegetation combine to give the largest spacing. If tree elements are removed, leaving only the buildings, the element spacing increases markedly at the vegetated sites. At residential sites the mean building spacing increases from about 40 to 65 m, and for individual sectors, which include wooded parks, values well in excess of 100 m are possible (e.g., C92w, Mi95, C95, and A94; Fig. A1e).

#### d. Roughness plan aspect ratio ( $\lambda_p$ )

For all sites except Arcadia (A94), buildings constitute a larger areal fraction of the roughness elements than do trees. The site means (trees and buildings) range from approximately 35% (T90, C95, Mi95, Sg94) to approximately 55% (S91, A94; Table 2). For individual sectors,  $\lambda_p$  ranges from as low as 20% (Mi95, Me93) to greater than 60% (S91, C92w, Me93; Fig. A1a). Omitting trees decreases  $\lambda_p$  by about 5%–10% at most residential sites, but the change can be greater than 30%

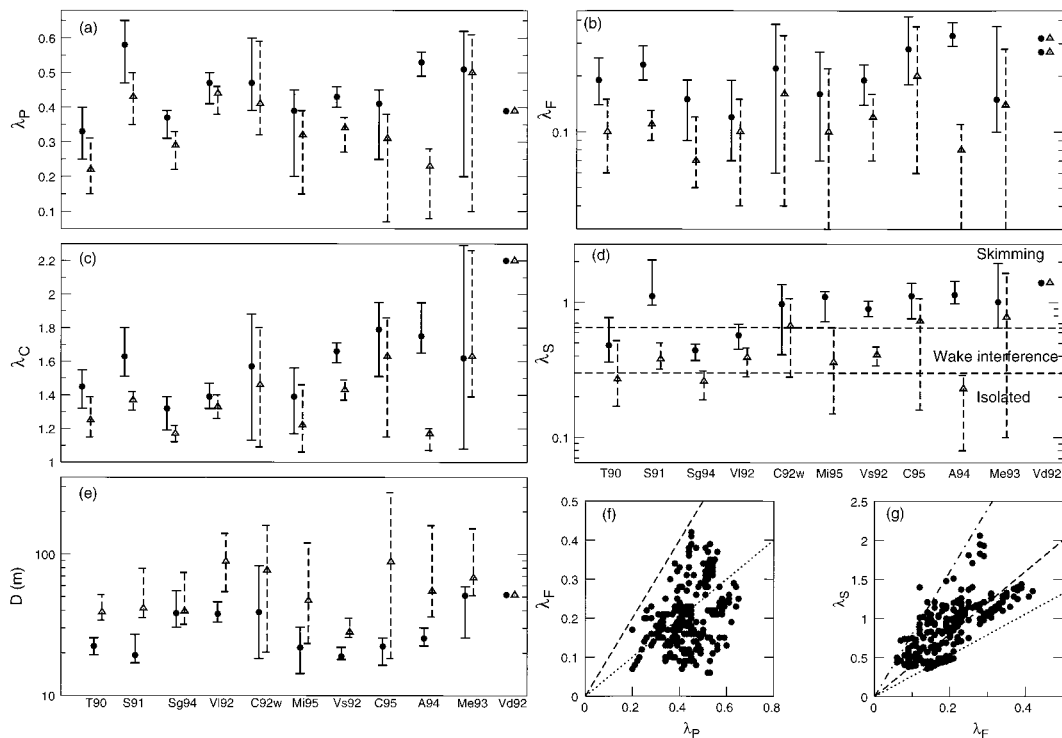


FIG. A1. The morphometric characteristics of 24  $15^\circ$  sectors, with dimensions determined by FSAM (for  $z_{ref}/L' = -0.04$ ), around each study site. The median (dot or triangle) and maximum and minimum (horizontal bars) values are shown. Triangles with dashed lines are values just for buildings; filled circles with solid lines are values for buildings and trees combined. In (a)–(e) the cities are arranged in order of increasing  $\bar{z}_H$  from left to right. (a) Plan area fraction  $\lambda_P$ ; (b) frontal area index  $\lambda_F$ ; (c) complete active surface area  $\lambda_C$ ; (d) canyon aspect (height:width) ratio  $\lambda_S$ ; (e) mean interelement spacing  $D$ ; (f)  $\lambda_P$  vs  $\lambda_F$ ; and (g)  $\lambda_P$  vs  $\lambda_S$  using data for all sectors for all cities. (f), (g) Lines shown are  $L_x = L_y = z_H$ , i.e., cubes (dashed lines);  $L_y = 2L_x = z_H$  (dotted lines); and  $L_x = L_y = 0.5 z_H$  (alternating dashed and dotted lines) with  $D_x$  and  $D_y$  kept constant. (f) Note that the last two cases plot on top of each other.

at a heavily wooded site (A94). Naturally, there is virtually no change at sparsely vegetated sites (V192, Me93, Vd92). The values for areal coverage of buildings cover a similar range to those reported for U.K. residential areas (Spanton et al. 1998).

#### e. Roughness frontal aspect ratio ( $\lambda_F$ )

The mean frontal area index of roughness elements (trees and buildings) at the sites studied is typically in the range from 0.1 to 0.3 with individual sectors varying from 0.06 to 0.4 (Fig. A1b; note that this figure has a logarithmic axis). For the residential set, the slightly higher values at S91, C92w, C95, and A94 are due to their greater tree cover. Inclusion of trees in the calculations increases the mean  $\lambda_F$  by more than a factor of 2 in some cities (S91, Vs92, Mi95) and up to a factor of 4 at A94. For the downtown site in Vancouver, the two points correspond to values determined at  $90^\circ$  to each other. The values for the Me93 site (which initially seem low) highlight the inability of the parameter  $\lambda_F$  to distinguish between certain distinct urban morphologies [i.e., similar values are derived for neighborhoods with small buildings of medium density and neighborhoods

with large (though not particularly tall) buildings of low (numerical) density].

#### f. Complete aspect ratio ( $\lambda_C$ )

The complete aspect ratio (Fig. A1c) is calculated using the method of Voogt and Oke (1997); it is the ratio of the complete surface area (the total three-dimensional area of vegetation and buildings) to the plan area. Hence, it gives an idea of the increase in the active surface–air interface due to the vertical dimensions of the city as compared with a flat area. For wind considerations it represents the relative increase in the potential momentum sink, but in reality not all of this increased area is effective (e.g., that area below the zero plane and where the flow is separated from the surface). The overall mean calculated for the residential areas is 1.57; at the lower end of the range are Sg94 and Mi95 (1.3), and at the upper end is A94 (1.8). When trees are excluded, as expected, values drop in Los Angeles by the greatest amount. For individual sectors,  $\lambda_C$  (buildings and trees) varies from less than 1.2 to slightly less than 2 (A94). As might be expected, the largest values (about 2.2) are for sectors in the high-rise commercial core of

Vd92. The old city core site of Me93 is extremely variable by sector. The ratio for the warehouse site VI92 is centered at about 1.4. While this value might be considered low, this site has very little tree cover so the extra area is attributable almost entirely to walls.

*g. Canyon aspect ratio ( $\lambda_s$ ) and related canyon properties*

The canyon aspect ratio, also known as the canyon height to street width ratio ( $\lambda_s = \overline{z_H}/\overline{W}$ ), is a fundamental property of surface morphometry and is used to provide a useful nondimensional scale in many urban climate applications (e.g., sky view factors for solar access and longwave radiation exchange, urban surface albedo, UCL heat island, classification of flow regimes, and canyon circulations, etc.). At the residential study sites, the mean  $\lambda_s$  values (including all roughness elements) range from about 0.4 (Sg94) to greater than 1.0 (S91 and A94; Fig. A1d). If trees are neglected,  $\lambda_s$  is significantly reduced at most sites. The central city sites have ratios that are large despite the lack of trees. These North American values cover a range similar to those presented by Theurer (1993) for German cities.

Central to the present study is the notion that flow regimes are altered in response to critical ratios of  $\lambda_s$ , as sketched in Fig. 1. When the limits suggested by Hussain and Lee (1980) are added to Fig. A1d, it shows that most residential sectors in these cities lie in the skimming flow regime (if both trees and buildings are considered), the exceptions being T90, Sg94, and parts of C92w. If the contribution of trees were to be removed from the calculation, the influence of buildings alone would put most sites in the wake interference regime and some even into isolated flow. This shift highlights the need to account for trees in any morphometric assessment of urban roughness.

*h. Relationship between geometric characteristics*

None of the morphometric parameters considered here fully captures the suite of morphometric characteristics needed to model aerodynamic parameters in urban areas. For example,  $\lambda_p$  does not respond to changes in height or the orientation of the roughness elements relative to the wind, and, if the total area covered by the roughness elements is the same, it may not distin-

guish neighborhoods with many small buildings from those with a few large (in terms of area) buildings. Similarly, although  $\lambda_F$  is a more sensitive measure to airflow, it fails to incorporate a measure of the alongwind dimensions of the roughness elements ( $L_x$ ) or the spaces between them ( $D_x - L_x$ ). Hence in the extreme case, a series of flat plates placed normal to the wind exert a large drag but apparently occupy almost no plan surface area (i.e.,  $\lambda_p$  approaches zero). Thus similar  $\lambda_F$  values may be obtained for sites with markedly different canyon aspect ratios ( $\lambda_s$ ).

Furthermore, it has to be recognized that in urban environments, with their wide array of building shapes and orientations, simple universal relations among  $\lambda_p$ ,  $\lambda_F$ , and  $\lambda_s$  just do not exist. Given the preceding remarks, it is perhaps not surprising to find that the two most commonly used descriptors of surface form for airflow ( $\lambda_p$  and  $\lambda_F$ ) do not correlate well with each other (Fig. A1f). Relations between descriptors like these depend on the relative dimensions of the buildings ( $L_x:L_y$ ) and their orientation relative to the wind. This is illustrated in Figs. A1f and A1g using three conditions:  $L_x = L_y = z_H$ , that is, cubes (dashed lines);  $L_y = 2L_x = z_H$  (dotted lines); and  $L_x = L_y = 0.5 z_H$  (alternating dashed and dotted lines) with  $D_x$  and  $D_y$  kept constant. Note that in Fig. A1f the last two conditions plot on top of each other. Clearly, real variations in geometry are more complex than cubes and other regular shapes and arrays, and vegetation further complicates these relations. The relation between  $\lambda_F$  and  $\lambda_s$  is better (Fig. A1g). This relationship is promising potentially in urban climate studies because together the two descriptors are represented in several successful aerodynamic, radiative, and thermal parameterizations. This finding may warrant further study.

## APPENDIX B

### Field Studies That Did Not Meet the Criteria for Acceptance

Table B1 gives a list of the studies reviewed for  $z_0$  and  $z_d$  data that *do not* fulfill the criteria for acceptance. For explanation of problem codes see Table B2. If a study failed two or more criteria, it was not considered further; that is, there may be additional problems than those listed here.

TABLE B1. Rejected studies, with locations and reasons for rejection. Problem codes are defined in Table B2.

Original citations	City (site name)	Problems
Ariel and Kliuchnikova (1960)	Kiev, Ukraine	Originally no $z_d$ —later modified, no land cover, $z_{\max}/z_{\min}$
Borisenko and Zavarina (1971)	Leningrad, Russia	No $z_0$ , no $z_d$ , no land cover
Bowne and Ball (1970)	Fort Wayne, IN (GT)	No $z_d$ , no land cover
Brook (1972)	Melbourne, Australia (Physics Dept., RMIT)	No $z_d$ , no land cover, stability
Coppin (1979)	Adelaide, Australia (Lw)	$z_d/z_H < 2$ , no land cover
Coppin (1979)	Adelaide, Australia (Ts)	No land cover, $z_d/z_H$ very low
Csanady et al. (1968)	Fort Wayne, IN (upwind edge of city)	No $z_d$ , no land cover
Davenport (1967)	London, Ontario, Canada (bell tower)	No $z_d$ , no land cover, no ht, $z_{\max}/z_{\min}$
Deland and Binkowski (1966)	Minneapolis, MN (KSTP-TV)	No $z_d$ , no land cover, sampling, no ht
Deland (1968)	Minneapolis, MN (KSTP-TV)	No $z_d$ , no land cover, stability, no ht
DeMarrais (1961)	Louisville, KY (WHAS)	No $z_0$ , no $z_d$ , no land cover
Dobbins (1977)	Cambridge, MA (MIT)	No $z_d$ , no land cover, $z_d/z_H < 2$ , sampling, inst
Duchêne-Marullaz (1975, 1980)	Nantes, France (CSTB)	Originally no $z_d$ —later modified, no land cover, no ht, (see Table 3 for modified and accepted values)
Feigenwinter et al. (1997)	Basel, Switzerland (BASTA 51 m)	No land cover, $z_d > z_H$ , $z_d/z_H < 2$
Graham (1968)	Fort Wayne, IN (Devoe, forest park, WANE TV)	No $z_0$ , no $z_d$ , no land cover, sampling, stability
Greaves (1962)	Minneapolis, MN (KSTP)	No $z_d$ , no land cover, no ht
Högström et al. (1982)	Uppsala, Sweden (Granby)	See Karlsson (1981, 1986) (see Table 3)
Högström et al. (1982)	Uppsala, Sweden (Upplandia)	See Karlsson (1981, 1986) (see Table 3)
Hu and Zhang (1993)	Tsukuba Science City, Japan (Meteorological Research Institute)	No $z_d$ , no land cover
Jackson (1978)	Wellington, New Zealand	Originally no $z_d$ —modified by Theurer but suspect relative to $z_H$
Jensen (1958, 1968), Jensen and Franck (1963)	Copenhagen, Denmark	Originally no $z_d$ —modified by Wieringa, $z_d/z_H < 2$ , no land cover, sampling, inst, stability
Jones et al. (1971)	Liverpool, United Kingdom	Originally no $z_d$ —modified by Theurer, $z_d/z_H < 2$ (see Table 3 for modified and accepted values)
Kawanabe (1964)	Tokyo, Japan (Tokyo tower)	No $z_d$ , no land cover, inst exp
Kimura and Takahashi (1991)	Tokyo, Japan	Not anemometric
Kondo and Yamazawa (1986)	Various Japanese cities	No $z_d$ , scale of whole city
Kono and Ito (1990)	Osaka, Japan	No $z_0$ , no $z_d$
Landsberg (1979)	Columbia, MD (built up, housing)	No $z_d$ , no land cover, sampling, no ht
Maisel (1971)	Columbia, MD (houses, parking lot, streets)	No $z_d$ , no land cover, $z_d/z_H < 2$ , stability, no ht
Pasquill (1970) after Marsh	Reading, United Kingdom	No $z_d$ , no land cover, sampling
McElroy and Pooler (1968)	Saint Louis, MO	No $z_0$ , no $z_d$ , no land cover
Miao and Ji (1996)	Tianjing City, China	No $z_d$ , no land cover
Mitani (1950)	Kawaguchi, Japan (urban)	No $z_d$ , no land cover
Myrup and Morgan (1972)	Sacramento, CA	Not anemometric
Nicholas and Lewis (1980)	Baltimore, MD	Not anemometric
Oikawa and Meng (1995)	Sapporo, Japan	Originally not anemometric—modified here (see Table 3)
Peschier (1973)	Austin, TX (site 1)	No $z_d$ , no land cover, $z_d/z_H < 2$ , no ht
Pooler (1963)	Saint Louis, MO	No $z_d$ , no land cover, no $z_0$
Rijkoort et al. (1970)	Rotterdam, the Netherlands	No $z_d$ , no land cover
Shellard (1968)	London, United Kingdom	$z_d/z_H < 2$ , no land cover, sampling, inst
Shiotani (1962)	Tokyo, Japan (Kokubunji)	No $z_d$ , $z_d/z_H < 2$ , no land cover
Shiotani and Yamamoto (1950)	Tokyo, Japan (Chiyoda-ku)	Originally no $z_d$ —later modified, no land cover
Shklyarevich (1974)	Leningrad, Russia (TV tower and Voyeykovo Station)	Inst, no land cover, stability
Slade (1969)	Philadelphia, PA (WFIL-WRCT-TV tower)	No $z_d$ , no land cover, terrain, no ht
Soma (1964)	Tokyo, Japan (Tokyo tower)	No $z_d$ , no land cover
Sponholz (1965)	Minneapolis, MN (KSTP-TV)	No $z_d$ , no land cover, no ht
Steyn (1982)	Vancouver, British Columbia, Canada (Sunset)	Not anemometric
Takahashi et al. (1981)	Ogaki City, Japan	Not anemometric
Teunissen (1977)	Ottawa, Ontario, Canada (suburban airport)	Mixture of suburban and nonurban fetch
Tsukamoto (1985, 1986), Yamamoto and Tsukamoto (1985)	Tsukuba Science City, Japan	No $z_0$ , no $z_d$ , no ht
Wamsler and Müller (1977)	Hamburg, Germany (docklands sector III)	No $z_d$ , no land cover, no ht
Xu et al. (1993)	Guangzhou, China (city center)	No land cover
Xu et al. (1997)	Nanjing, China (NJU)	No land cover, $z_d/z_H < 2$
Yamamoto and Shimanuki (1964)	Tokyo, Japan (Tokyo tower Minato-ku)	No $z_d$ , no land cover, no ht

TABLE B2. Explanation of problem codes from Table B1.

Code	Problem	Code	Problem
Terrain	Relief in area of concern	Stability	Not neutral or stability not considered
Fetch	Insufficient or inappropriate fetch	No $z_d$	The $z_d$ not included in analysis
Inst	Instrument details not given	No $z_0$	The $z_0$ not provided
Inst exp	Instrument exposure of concern	Sampling	Sampling details not given
No ht	No height information	$z_s/z_H < 2$	Lowest sensor level $< 2 z_H$
No land cover	Land cover information not given	$z_{smax}/z_{smin}$	The $z_{smax}/z_{smin}$ not greater than 2

APPENDIX C

Symbols, Subscripts, and Abbreviations

a. Symbols

- $A_F$  Frontal area of roughness elements ( $m^2$ ).
- $A_p$  Plan area of roughness elements ( $m^2$ ).
- $A_T$  Plan area of total surface ( $m^2$ ).
- $C_d, C_D$  Drag coefficient (-).
- $D$  Horizontal distance between centers of consecutive roughness elements (m).
- $L$  Horizontal dimension of roughness element (m).
- $L'$  Obukhov length (m).
- $U$  Large-scale wind speed ( $m s^{-1}$ ).
- $W$  Horizontal distance between vertical facets of consecutive elements (spacing) (m).
- $C_{d1}$  Free parameter.
- $C_R$  Drag coefficient of an isolated roughness element.
- $C_S$  Drag coefficient for substrate surface at  $z_H$ .
- $f$  Empirical coefficient used in Rt, Pa, and Ga formulas.
- $g_{aM}$  Aerodynamic conductance for momentum ( $mm s^{-1}$ ).
- $k$  von Kármán's constant (0.4).
- $p$  porosity of roughness elements (-).
- $u$  horizontal wind speed ( $m s^{-1}$ ).
- $u_*$  friction velocity ( $m s^{-1}$ ).
- $w_i$  FSAM source area weight for pixel located at sector  $i$ .
- $z_0$  Aerodynamic roughness length for momentum (m).
- $z_d$  Zero-plane displacement length (m).
- $z_H$  Height of roughness element (m).
- $z_r$  Blending height (m).
- $z_s$  Sensor height (m).
- $z_{ref}$  Reference height ( $= z_s - z_d$ ) (m).
- $\alpha$  Empirical coefficient in Ma equation for  $z_d$ .
- $\beta$  Empirical coefficient in Ma equation for  $z_0$ .
- $\delta$  Boundary layer height (m).
- $\lambda_C$  Complete, or three-dimensional aspect ratio ( $m^2 m^{-2}$ ).
- $\lambda_F$  Frontal area aspect ratio, roughness density ( $m^2 m^{-2}$ ).
- $\lambda_p$  Plan area aspect ratio, roughness density ( $m^2 m^{-2}$ ).
- $\lambda_S$  Street canyon aspect ratio ( $m m^{-1}$ ).
- $\lambda_x$  Either  $\lambda_F$  or  $\lambda_p$ .

- $\rho_a, \rho_{el}$  Density of air and roughness elements ( $m^{-2}$ ), respectively.
- $\sigma_H$  Standard deviation of roughness element height (m).
- $\sigma_v$  Horizontal crosswind standard deviation of wind speed ( $m s^{-1}$ ).
- $\tau_0$  Turbulent flux of horizontal momentum (Pa).
- $\varphi$  wind direction ( $^\circ$ ).
- $\psi$  Roughness sublayer influence function (-).

b. Subscripts

- $b$  Buildings.
- $d, 0, r$  Coefficients or methods related to  $z_d, z_0,$  or  $z_r,$  respectively.
- $i$  Individual roughness elements.
- $t$  Trees.
- $x, y, z$  Alongwind, crosswind, and vertical directions, respectively.

c. Abbreviations

- Ba Bottema Eqs. (9) and (10).
- Bo Bottema Eq. (18) and Table 1.
- Co Counihan Eqs. (5)–(7).
- Ga Garratt Eq. (19).
- Ko Kondo and Yamazawa Eq. (8).
- Ku Kutzbach Eqs. (3) and (4).
- Le Lettau Eq. (12).
- Ma Macdonald et al. Eqs. (13) and (14).
- Mu Mulhearn and Finnigan Eq. (20).
- Pa Pasquill Eq. (19).
- Ra Raupach Eqs. (15), (16), and (21).
- Rt Rule-of-thumb Eqs. (1) and (2).

REFERENCES

Angell, J. K., W. H. Hoecker, C. R. Dickson, and D. H. Pack, 1973: Urban influence on a strong daytime air flow as determined from tetroon flights. *J. Appl. Meteor.*, **12**, 924–936.

Ariel, M. Z., and L. A. Kliuchnikova, 1960: Wind over a city. *Tr. Gl. Geofiz. Obs.*, **94**, 29–32.

Auer, A. H., Jr., 1981: The urban boundary layer. *Meteor. Monogr.*, No. 40, Amer. Meteor. Soc., 41–62.

Borisenko, M. M., and M. V. Zavarina, 1971: Peculiarities of the wind regime and the lower layer of the atmosphere above a city. *Tr. Gl. Geofiz. Obs.*, **283**, 12–21.

Bottema, M., 1995a: Aerodynamic roughness parameters for homogeneous building groups—Part 1: Theory. Document SUB-MESO 18, Ecole Centrale de Nantes, France, 40 pp. [Available from Equipe Dynamique de l'Atmosphère Habitée, Laboratoire de Mécanique des Fluides, Ecole Centrale de Nantes, 1 rue de la Noë, 44072 Nantes Cedex 03, France.]

- , 1995b: Aerodynamic roughness parameters for homogeneous building groups—Part 2: Results Document SUB-MESO 23, Ecole Centrale de Nantes, France, 80 pp. [Available from Equipe Dynamique de l'Atmosphère Habitée, Laboratoire de Mécanique des Fluides, Ecole Centrale de Nantes, 1 rue de la Noë, 44072 Nantes Cedex 03, France.]
- , 1995c: Parameterisation of aerodynamic roughness parameters in relation to air pollutant removal efficiency of streets. *Air Pollution Engineering and Management*, H. Power et al., Eds., Computational Mechanics, 235–242.
- , 1997: Urban roughness modelling in relation to pollutant dispersion. *Atmos. Environ.*, **31**, 3059–3075.
- Bowne, N. E., and J. T. Ball, 1970: Observational comparison of rural and urban boundary layer turbulence. *J. Appl. Meteor.*, **9**, 862–873.
- Brook, R. R., 1972: Measurements of turbulence in a city environment. *J. Appl. Meteor.*, **11**, 443–450.
- Cermak, J. E., A. G. Davenport, E. J. Plate, and D. X. Viegas, Eds., 1995: *Wind Climate in Cities*. Kluwer Academic, 772 pp.
- Cionco, R. M., and R. Ellefsen, 1998: High resolution urban morphology data for urban wind flow modeling. *Atmos. Environ.*, **32**, 7–17.
- Clarke, J. F., J. K. S. Ching, and J. M. Godowitch, 1982: An experimental study of turbulence in an urban environment. Tech. Rep. EPA 600/3-82-062, U.S. Environmental Protection Agency, Research Triangle Park, NC, 150 pp. [Available from Environmental Sciences Research Laboratory, U.S. Environmental Protection Agency, Research Triangle Park, NC 27711.]
- Claussen, M., 1995: Estimation of regional heat and moisture fluxes in homogeneous terrain with bluff body roughness elements. *J. Hydrol.*, **166**, 353–369.
- Cook, N. J., 1976: Data for wind tunnel simulation of the adiabatic atmospheric boundary layer. Part A, B, D. BRE Note 103/76, Building Research Establishment, Garston, Watford, United Kingdom.
- Coppin, P. A., 1979: Turbulent fluxes over a uniform urban surface. Ph.D. thesis, The Flinders University of South Australia, Research Rep. 31, 196 pp (unpublished). [Available from Flinders Institute for Atmospheric and Marine Sciences, The Flinders University of South Australia, Adelaide, Australia.]
- Counihan, J., 1971: Wind tunnel determination of the roughness length as a function of fetch and density of three-dimensional roughness elements. *Atmos. Environ.*, **5**, 637–642.
- Csanady, G. T., G. R. Hilst, and N. E. Bowne, 1968: Turbulent diffusion from a cross-line source in a shear flow at Fort Wayne, Indiana. *Atmos. Environ.*, **2**, 273–292.
- Davenport, A. G., 1960: Rationale for determining design wind velocities. *J. Struct. Div. Amer. Soc. Civ. Eng.*, **86**, 39–68.
- , 1967: Instrumentation and measurement of wind spectra in a city. *Proc. Canadian Conf. on Micrometeorology*, Vol. 1, Toronto, ON, Canada, Meteorological Branch, Canada Department of Transport, 361–369.
- Deland, R. J., 1968: A study of atmospheric turbulence over a city. Final Report to U.S. Public Health Service, School of Engineering and Science, New York University, University Heights, NY. [Available from School of Engineering and Science, New York University, University Heights, NY 10453.]
- , and F. S. Binkowski, 1966: Comparison of wind at 500 feet over Minneapolis and Louisville with geostrophic wind. *J. Air Pollut. Control Assoc.*, **16**, 407–411.
- DeMarras, G. A., 1961: Vertical temperature difference observed over an urban area. *Bull. Amer. Meteor. Soc.*, **42**, 548–554.
- Dobbins, R. A., 1977: Observations of the barotropic Ekman layer over an urban area. *Bound.-Layer Meteor.*, **11**, 39–54.
- Duchêne-Marullaz, P., 1975: Full scale measurements of atmospheric turbulence in a suburban area. *Proc. Fourth Int. Conf. on Wind Effects on Buildings and Structures*, K. J. Eaton, Ed., Cambridge University Press, 23–31.
- , 1980: Effect of high roughness on the characteristics of turbulence in cases of strong winds. *Proceedings, Fifth Int. Conf. on Wind Engineering*, J. E. Cermak, Ed., Vol. 1, Pergamon Press, 179–193.
- Ellefsen, R., 1990–91: Mapping and measuring buildings in the canopy boundary layer in ten U.S. cities. *Energy Build.*, **15–16**, 1025–1049.
- Fang, C., and B. L. Sill, 1992: Aerodynamic roughness length: Correlation with roughness elements. *J. Wind Eng. Indus. Aerodyn.*, **41–44**, 449–460.
- Fazu, C., and P. Schwerdtfeger, 1989: Flux gradient relationships for momentum and heat over a rough natural surface. *Quart. J. Roy. Meteor. Soc.*, **115**, 335–352.
- Feigenwinter, C., R. Vogt, and E. Parlow, 1997: Vertical structure of turbulence above an urban canopy. Preprints, *12th Conf. on Boundary Layers and Turbulence*, Vancouver, BC, Canada, Amer. Meteor. Soc., 472–473.
- Garratt, J. R., 1978: Transfer characteristics for a heterogeneous surface of large aerodynamic roughness. *Quart. J. Roy. Meteor. Soc.*, **104**, 199–211.
- , 1980: Surface influence upon vertical profiles in the atmospheric near-surface layer. *Quart. J. Roy. Meteor. Soc.*, **106**, 803–819.
- , 1992: *The Atmospheric Boundary Layer*. Cambridge University Press, 316 pp.
- Graham, I. R., 1968: An analysis of turbulence statistics at Fort Wayne, Indiana. *J. Appl. Meteor.*, **7**, 90–93.
- Greaves, J. T., 1962: Surface wind structure over a city. M.S. thesis, University of Minnesota, 37 pp.
- Grimmond, C. S. B., and T. R. Oke, 1991: An evapotranspiration-interception model for urban areas. *Water Resour. Res.*, **27**, 1739–1755.
- , and C. Souch, 1994: Surface description for urban climate studies: A GIS based methodology. *Geocarto Int.*, **9**, 47–59.
- , and T. R. Oke, 1995: Comparison of heat fluxes from summertime observations in the suburbs of four North American cities. *J. Appl. Meteor.*, **34**, 873–889.
- , and —, 1998: Heat storage in urban areas: Observations and evaluation of a simple model. *J. Appl. Meteor.*, **38**, 922–940.
- , T. S. King, M. Roth, and T. R. Oke, 1998: Aerodynamic roughness of urban areas derived from wind observations. *Bound.-Layer Meteor.*, **89**, 1–24.
- Hanna, S. R., and J. C. Chang, 1992: Boundary layer parameterisations for applied dispersion modelling over urban areas. *Bound.-Layer Meteor.*, **58**, 229–259.
- Heisler, G. M., 1984: Measurements of solar radiation on vertical surfaces in the shade of individual trees. *The Forest-Atmosphere Interaction*, B. A. Hutchinson and B. B. Hicks, Eds., D. Reidel, 319–335.
- , and D. R. DeWalle, 1988: Effect of wind break structure on wind flow. *Agric. Ecosyst., Environ.*, **22–23**, 41–69.
- Hicks, B. B., 1973: Eddy fluxes over a vineyard. *Agric. Meteor.*, **12**, 203–215.
- , and R. P. Hosker Jr., 1987: Dry deposition of air pollutants in an urban environment. *Modeling the Urban Boundary Layer*, Amer. Meteor. Soc., 411–428.
- Högström, U., H. Bergström, and H. Alexandersson, 1982: Turbulence characteristics in a near neutrally stratified urban atmosphere. *Bound.-Layer Meteor.*, **23**, 449–472.
- Hu, Y., and Q. Zhang, 1993: On local similarity of the atmospheric boundary layer. *Sci. Atmos. Sin.*, **17**, 10–20.
- Hussain, M., and B. E. Lee, 1980: A wind tunnel study of the mean pressure forces acting on large groups of low-rise buildings. *J. Wind Eng. Ind. Aerodyn.*, **6**, 207–225.
- Iqbal, M., A. K. Khatry, and B. Seguin, 1977: A study of the roughness effects of multiple windbreaks. *Bound.-Layer Meteor.*, **11**, 197–203.
- Jackson, P. S., 1978: Wind structure near a city centre. *Bound.-Layer Meteor.*, **15**, 323–340.
- , 1981: On the displacement height in the logarithmic velocity profile. *J. Fluid Mech.*, **111**, 15–25.

- Jensen, M., 1958: The model law for phenomena in natural wind. *Ingeniøren*, **2**, 121–128.
- , 1968: Some lessons learned in building aerodynamic research. *Proc. Int. Research Sem. on Wind Effects on Buildings and Structures*, Vol. 1, Ottawa, ON, Canada, University of Toronto Press, 1–18.
- , and N. Franck, 1963: *Model Scale Tests in Turbulent Wind: Parts 1 and 2*. Danish Technical Press, 97 pp.
- Jones, P. M., M. A. B. deLarrinaga, and C. B. Wilson, 1971: The urban wind velocity profile. *Atmos. Environ.*, **5**, 89–102.
- Karlsson, S., 1981: Analysis of wind profile data from an urban–rural interface site. Rep. 58, Department of Meteorology, University of Uppsala. [Available from Meteorology, Earth Science Centre, University of Uppsala, Uppsala, Sweden.]
- , 1986: The applicability of wind profile formulas to an urban–rural interface site. *Bound.-Layer Meteor.*, **34**, 333–355.
- Kawanabe, Y., 1964: Vertical wind profile below 300 m. *Kobe Kaiyo Kishodai Iho*, **172**, 93–118.
- Kimura, F., and S. Takahashi, 1991: The effects of land-use and anthropogenic heating of the surface temperature in the Tokyo metropolitan area: A numerical experiment. *Atmos. Environ.*, **25B**, 155–164.
- Kondo, J., and H. Yamazawa, 1986: Aerodynamic roughness over an inhomogeneous ground surface. *Bound.-Layer Meteor.*, **35**, 331–348.
- Kono, H., and S. Ito, 1990: A micro-scale dispersion model for motor vehicle exhaust gas in urban areas—OMG volume-source model. *Atmos. Environ.*, **24B**, 243–251.
- Kratzer, P. A., 1956: *Das Stadtklima (The Urban Climate)*. 2d ed. Friedr. Vieweg und Sohn, 184 pp.
- Kutzbach, J., 1961: Investigations of the modifications of wind profiles by artificially controlled surface roughness. M.S. thesis, Department of Meteorology, University of Wisconsin—Madison, 58 pp.
- Landsberg, H. E., 1979: Atmospheric changes in a growing community. *Urban Ecol.*, **4**, 53–81.
- , 1981: *The Urban Climate*. Academic Press, 275 pp.
- Lettau, H., 1969: Note on aerodynamic roughness parameter estimation on the basis of roughness element description. *J. Appl. Meteor.*, **8**, 828–832.
- Liedtke, J., 1992: Experimentelle Untersuchung des Ausbreitungsverhaltens eines gasförmigen Stoffes in neutral und instabil geschichteten turbulenten Gleichdruckgrenzschichten bei unterschiedlicher Bodenrauigkeit (An experimental investigation into the dispersion behavior in neutral and unstable zero pressure gradient boundary layers with different roughnesses). Ph.D. thesis, Universität der Bundeswehr, München, Germany, 179 pp. [Available from Federated Armed Forces University, Munich, Institute for Fluid Mechanics and Aerodynamics, Universität Bundeswehr, Werner-Heisenberg-Weg 39, 85577 Neubiberg, Germany.]
- Macdonald, R. W., R. F. Griffiths, and D. J. Hall, 1998: An improved method for estimation of surface roughness of obstacle arrays. *Atmos. Environ.*, **32**, 1857–1864.
- Maisel, T. N., 1971: Early micrometeorological changes caused by urbanization. M.S. thesis, Institute for Fluid Dynamics and Applied Mathematics, University of Maryland, 50 pp. [Available from Institute for Dynamics and Applied Mathematics, University of Maryland, College Park, MD 20742.]
- McElroy, J. L., and F. Pooler, 1968: St. Louis dispersion study. Vol. 2. Analysis. U.S. Department of Health, Education, and Welfare, National Air Pollution Control Administration, Arlington, VA, 51 pp. [Available from U.S. Government Printing Office, Washington, DC 20402.]
- Miao, M., and J. Ji, 1996: Study of diurnal variation of bulk drag coefficient over different land surfaces. *Meteor. Atmos. Phys.*, **61**, 217–224.
- Mitani, I., 1950: Report of wind observations on Kawaguchi wireless tower. *J. Meteor. Res. Tokyo*, **2**, 310–318.
- Mulhearn, P. J., 1978: Turbulent flow over a periodic rough surface. *Phys. Fluids*, **21**, 1113–1115.
- , and J. J. Finnigan, 1978: Turbulent flow over a very rough, random surface. *Bound.-Layer Meteor.*, **15**, 109–132.
- Myrup, L. O., and D. L. Morgan, 1972: Numerical model of the urban atmosphere. *The City-Surface Interface, Contributions in Atmospheric Science*, Vol. 1, Department of Agriculture Engineering and Water Science Engineering, University of California, Davis, 237 pp.
- Newberry, C. W., and J. K. Eaton, 1974: *Wind Loading Handbook*. HMSO, 74 pp.
- Nicholas, F. W., and J. E. Lewis Jr., 1980: Relationships between aerodynamic roughness and land use and land cover in Baltimore, Maryland. Geological Survey Prof. Paper 1099-C, U.S. Govt. Printing Office, Washington, D.C., 36 pp. [Available from U.S. Government Printing Office, Washington, DC 20402.]
- Oikawa, S., and Y. Meng, 1995: Turbulence characteristics and organized motion in a suburban roughness layer. *Bound.-Layer Meteor.*, **74**, 289–312.
- Oke, T. R., 1987: *Boundary Layer Climates*. 2d ed. Routledge, 435 pp.
- O’Loughlin, E. M., and E. G. MacDonald, 1964: Some roughness concentration effects on boundary layer resistance. *La Houille Blanche*, **7**, 773–782.
- Pasquill, F., 1970: Prediction of diffusion over an urban area—Current practice and future prospects. *Proceedings of Symposium on Multiple-Source Urban Diffusion Models*, A. C. Stern, Ed., U.S. Environmental Protection Agency, 3-1–3-26.
- , 1974: *Atmospheric Diffusion*. 2d ed. Wiley, 429 pp.
- Peschier, J., 1973: Wind and temperature profiles in an urban area. Rep. 33, Atmospheric Science Group, University of Texas at Austin, 32 pp.
- Petersen, R. L., 1997: A wind tunnel evaluation of methods for estimating surface roughness length in industrial facilities. *Atmos. Environ.*, **31**, 45–57.
- Pooler, F., 1963: Airflow over a city in terrain of moderate relief. *J. Appl. Meteor.*, **2**, 446–456.
- Rafailidis, S., 1997: Influence of building, areal density and roof shape on the wind characteristics above a town. *Bound.-Layer Meteor.*, **85**, 255–271.
- Raupach, M. R., 1992: Drag and drag partition on rough surfaces. *Bound.-Layer Meteor.*, **60**, 375–395.
- , 1994: Simplified expressions for vegetation roughness length and zero-plane displacement as functions of canopy height and area index. *Bound.-Layer Meteor.*, **71**, 211–216.
- , 1995: Corrigenda. *Bound.-Layer Meteor.*, **76**, 303–304.
- , and B. J. Legg, 1984: The uses and limitations of flux-gradient relationships in micrometeorology. *Agric. Water Manage.*, **8**, 119–131.
- , A. S. Thom, and I. Edwards, 1980: A wind tunnel study of turbulent flow close to regularly arrayed rough surfaces. *Bound.-Layer Meteor.*, **18**, 373–397.
- , R. A. Antonia, and S. Rajagopalan, 1991: Rough wall turbulent boundary layers. *Appl. Mech. Rev.*, **44**, 1–25.
- Rijkoort, P. J., F. H. Schmidt, C. A. Velds, and J. Wieringa, 1970: A meteorological 80 m tower near Rotterdam. *Bound.-Layer Meteor.*, **1**, 5–17.
- Rotach, M. W., 1994: Determination of the zero plane displacement in an urban area. *Bound.-Layer Meteor.*, **67**, 187–193.
- Roth, M., 1998: Review of atmospheric turbulence over cities. *Quart. J. Roy. Meteor. Soc.*, in press.
- Schaudt, K. J., 1998: A new method for estimating roughness parameters and evaluating the quality of observations. *J. Appl. Meteor.*, **37**, 470–476.
- Schlichting, H., 1937: Experimental investigation of the problem of surface roughness. *Exp. Untersuchungen Rauigkeitsproblem Ingenieur-Archiv*, **7**, 1–34.
- , 1968: *Boundary-Layer Theory*. 3d ed. McGraw-Hill, 747 pp.
- Schmid, H. P., 1994: Source areas for scalars and scalar fluxes. *Bound.-Layer Meteor.*, **67**, 293–318.

- Shaw, R. H., and A. R. Pereira, 1982: Aerodynamic roughness of a plant canopy: A numerical experiment. *Agric. Meteor.*, **26**, 51–65.
- Shellard, H. C., 1968: Results of some recent special measurements in the United Kingdom relevant to wind loading parameters. *Proc. Int. Research Seminar on Wind Effects on Buildings and Structures*, Vol. 2, Ottawa, ON, Canada, University of Toronto Press, 515–533.
- Shiotani, M., 1962: The relationship between wind profiles and stabilities of the air layer in outskirts of a city. *J. Meteor. Soc. Japan*, **40**, 315–329.
- , and G. Yamamoto, 1950: Atmospheric turbulence over the large city—Turbulence in the free atmosphere. *Geophys. Mag. Cent. Meteor. Observ. Japan*, **21**, 134–147.
- Shklyarevich, O. B., 1974: Peculiarities of vertical wind distribution and temperature under city conditions. *Meteor. I Gidrol.*, **7**, 42–46.
- Slade, D. H., 1969: Wind measurement on a tall tower in rough and inhomogeneous terrain. *J. Appl. Meteor.*, **8**, 293–297.
- Soma, S., 1964: The properties of atmospheric turbulence in high winds. *J. Meteor. Soc. Japan*, **42**, 372–396.
- Spanton, A. M., D. J. Hall, and S. Walker, 1998: A survey of the aerodynamic characteristics of some UK urban area. BRE Rep. CR 177/96, Building Research Establishment, Garston, United Kingdom, 21 pp. [Available from Building Research Establishment, Bucknall Lane, Garston, Watford WD2 7JR, United Kingdom.]
- Sponholz, M. P., 1965: Wind structure 50 to 150 meters above an urban area. M.S. thesis, Department of Meteorology, University of Wisconsin, 28 pp.
- Stewart, J. B., 1984: Measurement and prediction of evaporation from forested and agricultural catchments. *Agric. For. Manag.*, **8**, 1–28.
- Steyn, D. G., 1982: Turbulence in an unstable surface layer over suburban terrain. *Bound.-Layer Meteor.*, **22**, 183–191.
- Stull, R. B., 1988: *Introduction to Boundary Layer Meteorology*. Kluwer Academic, 666 pp.
- Styles, J. M., 1997: A wind tunnel study of the velocity field above a model plant canopy. CSIRO Land and Water Tech. Rep. 36–97, 67 pp.
- Szeicz, G., 1974: Gaseous wastes and the vegetation. Unpublished manuscript given at Symposium on Waste Recycling and the Environment, Royal Society of Canada, Ottawa, ON, Canada, 12 pp. [Available from Royal Society of Canada, 225 Metcalf St., Ottawa, ON K2P 1P9 Canada.]
- Takahashi, M., K. Sekine, T. Iwata, Y. Kosaka, and S. Fukawabi, 1981: The roughness parameter in Ogaki City. *Geogr. Rev. Japan*, **54**, 579–594.
- Taylor, P. A., 1987: Comments and further analysis on the effective roughness length for use in numerical three-dimensional models: A research note. *Bound.-Layer Meteor.*, **39**, 403–418.
- , 1988: Turbulent wakes in the atmospheric boundary layer. *Flow and Transport in the Natural Environment: Advances and Applications*, W. L. Steffen and O. T. Denmead, Eds., Springer-Verlag, 270–292.
- Teunissen, H. W., 1977: Measurements of planetary boundary layer wind and turbulence over a small suburban airport. Internal Report. MSRB-77-4, Atmospheric Environment Service, Toronto, ON, Canada, 45 pp. [Available from Atmospheric Environment Service, 4905 Dufferin St., Downsview, ON M3H 5T4 Canada.]
- Theurer, W., 1993: Ausbreitung bodennaher Emissionen in komplexen bebauungen (Dispersion of near ground emissions in complex building arrangements). Ph.D. thesis, IHW University of Karlsruhe, Germany, 206 pp. [Available from Institut für Hydrologie und Wasserwirtschaft, Universität Karlsruhe, Kaiserstrasse 12, D-76128 Karlsruhe, Germany.]
- Tieleman, H. W., T. A. Reinhold, and R. D. Marshall, 1978: On the wind tunnel simulation of the atmospheric surface layer for the study of wind loads on low-rise buildings. *J. Ind. Aerodyn.*, **3**, 21–28.
- Tsukamoto, O., 1985: Turbulence measurements of the planetary boundary layer from a 213 m meteorological tower. *Bull. Disaster Prev. Res. Inst. Kyoto Univ.*, **35**, 87–113.
- , 1986: Experimental study of heat and water vapor transfer processes in the planetary boundary layer. *Bound.-Layer Meteor.*, **35**, 349–368.
- Visser, G. Th., 1987: Modelontwikkeling voor de berekening van ventilatie-verliezen in wijken bestaande uit identieke bouwgroepverkavelingen. (Model development for the evaluation of ventilation losses in urban districts consisting of identical building groups). Rep. 87-104, TON-IMET-ST, Apeldoorn, Netherlands, 111 pp. [Available from TNO, Postbus 342, 7300 A. H. Apeldoorn, Netherlands.]
- Voogt, J. A., and T. R. Oke, 1997: Complete urban surface temperatures. *J. Appl. Meteor.*, **36**, 1117–1132.
- Wamser, C., and H. Müller, 1977: On the spectral scale of wind fluctuations within and above the surface layer. *Quart. J. Roy. Meteor. Soc.*, **103**, 721–720.
- Wieringa, J., 1992: Updating the Davenport roughness classification. *J. Wind Eng. Ind. Aerodyn.*, **41**, 357–368.
- , 1993: Representative roughness parameters for homogeneous terrain. *Bound.-Layer Meteor.*, **63**, 323–363.
- Willmott, C. J., 1981: On the validation of models. *Phys. Geogr.*, **2**, 184–194.
- Xu, Y., C. Zhao, Z. Li, and Z. Wei, 1993: Microstructure and spectral characteristics of turbulence in the surface layer atmosphere over Ghang Zhou. *Sci. Atmos. Sin.*, **17**, 338–348.
- , —, —, and —, 1997: Turbulent structure and local similarity in the tower layer over the Nanjing area. *Bound.-Layer Meteor.*, **82**, 1–21.
- Yamamoto, G., and A. Shimanuki, 1964: Profiles of wind and temperature in the lowest 250 meters in Tokyo. Scientific Rep. Tohoku University, Geophysics Series, **15**, 111–114.
- , and O. Tsukamoto, 1985: Turbulence in the atmospheric boundary layer: Generation and maintenance of turbulent kinetic energy. *Recent Studies in Turbulent Phenomena*, T. Tatsumi, H. Maruo, and H. Takami, Eds., Association for Science Documents Information.
- Yersel, M., and R. Goble, 1986: Roughness effects on urban turbulence parameters. *Bound.-Layer Meteor.*, **37**, 171–184.